Mitt. Österr. Geol. Ges. | ISSN 0251-7493 | 94 (2001) | 99-122 | Wien, August 2003

Keywords
Adula
Penninic nappes
Subduction
Exhumation
Eclogite

Structural evolution of Adula nappe, Misox zone, and Tambo nappe in the San Bernardino area: Constraints for the exhumation of the Adula eclogites

JAN PLEUGER[1], RENÉ HUNDENBORN[1], KERSTIN KREMER[1], SLAVICA BABINKA[1], WALTER KURZ[1], EKKEHARD JANSEN[2] & NIKOLAUS FROITZHEIM[1]

13 Figures and 1 Table

Content

Abstract

The Misox zone in the Central Alps is formed by metasediments and metavolcanics from the Valais ocean basin. It separates the underlying Adula nappe, derived from the distal European continental margin, dominated by pre-Mesozoic basement, and including Tertiary-age eclogites, from the overlying, eclogite-free Tambo basement nappe of Briançonnais origin. These three units were emplaced on each other during pervasive, top-north directed mylonitic shearing, termed Zapport-phase in the Adula nappe and Ferrera phase in the Misox zone and Tambo nappe. In the Adula nappe, the Zapport phase deformation occurred at ca. 35 Ma and was preceded by (1) subduction-related imbrication of basement and sediments and (2) eclogite-facies mylonitisation. Neutron diffractometry of five samples of eclogite mylonite from the Adula nappe yielded omphacite textures indicative of constrictional strain. The Zapport phase is postdated by top-east shearing during the Niemet-Beverin phase (35 to 30 Ma), which in the Adula nappe is very weak and only detectable from quartz textures, but becomes stronger towards the upper part of the Misox zone and in the Tambo nappe.

The main exhumation of the Adula eclogites, from ca. 20 kbar to ca. 7 kbar, occurred before and during the Zapport phase. The southward-increasing pressure gap existing between the Adula nappe and the Tambo nappe is explained by a Briançonnais lower crustal and mantle wedge originally situated between the Adula nappe below and the Tambo nappe above. When this wedge sank off into the asthenosphere, the Adula nappe was exhumed from below into the top-north Zapport shear zone.

Address of the authors

[1] Jan PLEUGER, René HUNDENBORN, Kerstin KREMER, Slavica BABINKA, Walter KURZ and Nikolaus FROITZHEIM, Geologisches Institut, Universität Bonn, Nussallee 8, D-53115 Bonn, Germany

[2] Ekkehard JANSEN, Mineralogisch-Petrologisches Institut, Universität Bonn, Poppelsdorfer Schloss, D-53115 Bonn, Germany

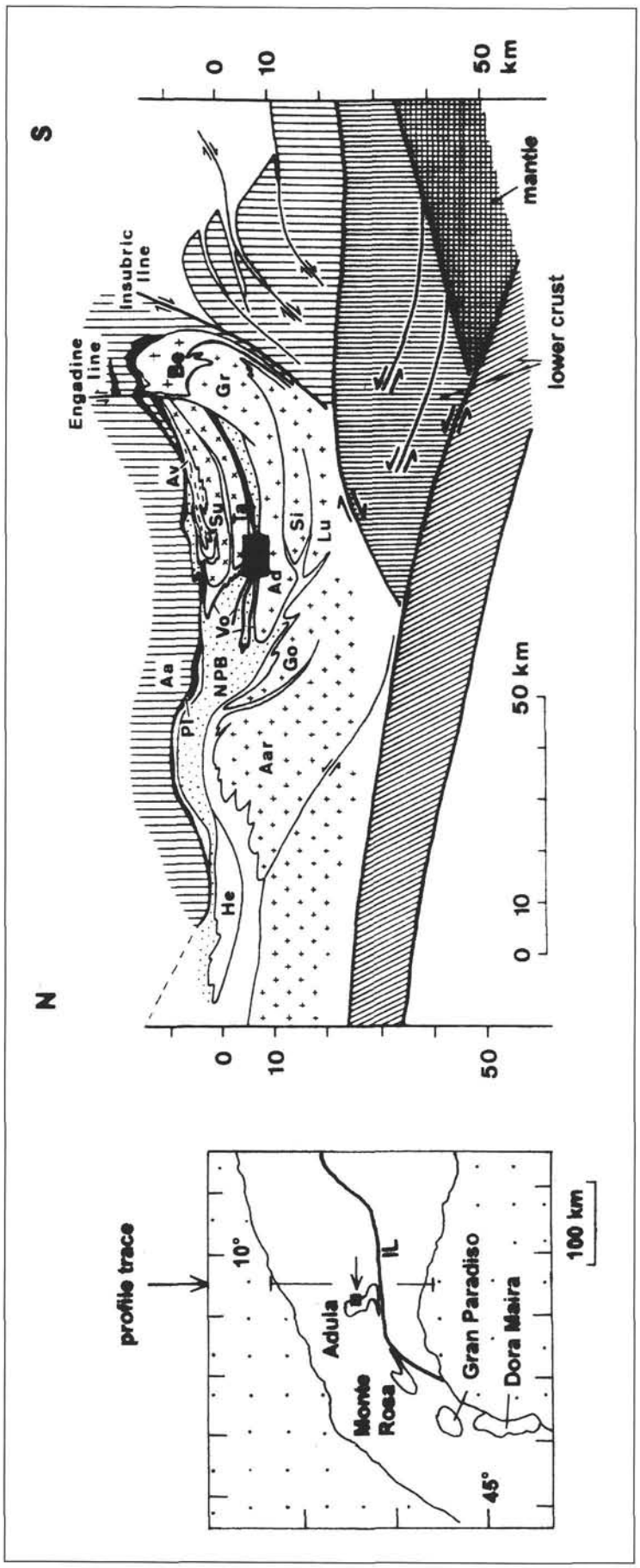

Fig. 1
Simplified map and cross-section of the central Alps. Map shows northern and southern foreland basins (stippled), Insubric line (IL), and European basement units with Tertiary high-pressure metamorphism (outlined). Cross section is from SCHMID et al. (1996) and shows European basement units (small crosses), Briançonnais basement nappes (small x pattern), ophiolites (black), sediments from the Valais basin (stippled), and Austroalpine/South Alpine units (vertical ruling). Aa: Austroalpine nappes; Ad: Adula nappe; Av: Avers Bündnerschiefer; Be: Bergell intrusion; Go: Gotthard „massif"; Gr: Gruf unit; He: Helvetic nappes; Lu: Lucomagno-Leventina nappe; NPB: North Penninic (Valaisan) Bündnerschiefer; Pl: Platta-Arosa nappe; Si: Simano nappe; Su: Suretta nappe; Ta: Tambo nappe; Vo: Valaisan ophiolites. Black quadrangles in map and cross-section indicate the study area.

1. Introduction

Tertiary-age, high-pressure and ultra-high-pressure metamorphic rocks including eclogites, metapelites, and garnet peridotites are found in the Adula nappe in the eastern Central Alps (Fig. 1). The peak metamorphic conditions of these increase from the northern end of the nappe (12 kbar/500 °C) to the southern end (32 kbar/840 °C), in accordance with the assumed southward subduction direction (HEINRICH 1986, BECKER 1993, NIMIS and TROMMSDORFF 2001, SCHMID et al. 1996). The Adula nappe is overlain by the Tambo nappe across the metasedimentary Misox zone, and underlain by the Simano nappe. Neither Tambo nor Simano include Alpine eclogite-facies rocks. Thus, the Adula nappe represents a high- to ultra-high pressure sheet emplaced between two lower-pressure sheets. Such emplacement, according to current models (CHEMENDA et al. 1995, ERNST 1999), would imply contemporaneous activity of a thrust at the base and a south-dipping normal fault at the top of the Adula nappe. To test the latter prediction, we conducted field and microstructural work in the middle Adula nappe and the units overlying it, the Misox zone and the Tambo nappe (Central Alps in eastern Switzerland, Figs. 1, 2). Our study corroborated earlier results (MEYRE and PUSCHNIG 1993, PARTZSCH 1998) that this zone is dominated by top-north shearing instead of the expected top-south normal faulting. The detailed structural analysis finally leads to a tectonic scenario that explains high-pressure exhumation in the framework of top-north directed shearing.

During field work the area from San Bernardino pass in the north to about 3 km south of the village San Bernardino was mapped (PLEUGER 2001, HUNDENBORN 2001, KREMER 2001, BABINKA 2001). It comprises the northern section of the Misox zone and adjacent parts of the underlying Adula

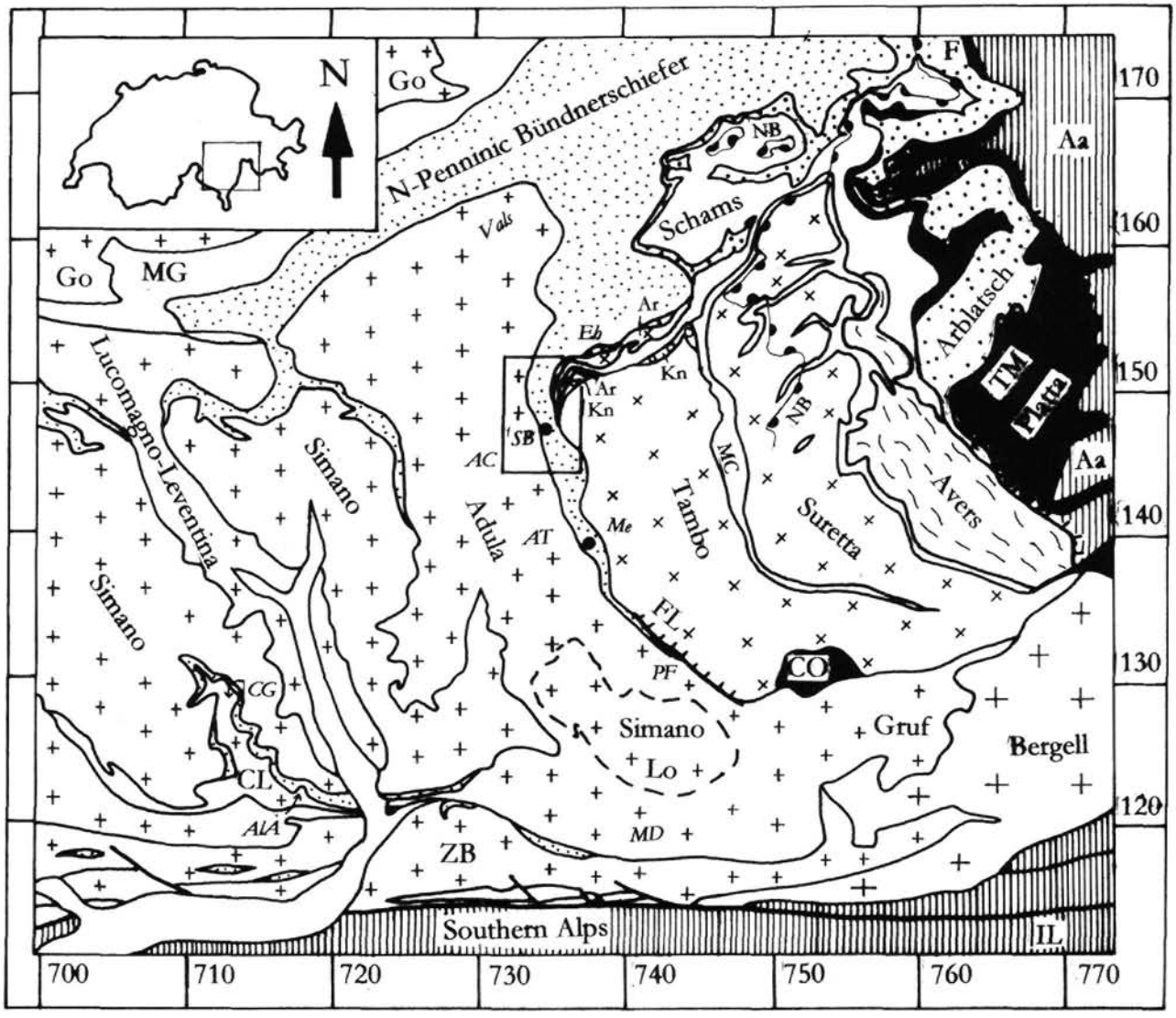

Fig. 2.
Tectonic overview of the eastern Lepontine area. Aa: Austroalpine units; Ar: Areua slice; CL: Cima Lunga unit; CO: Chiavenna ophiolite; F: Flysch; FL: Forcola Line, Go: Gotthard "massif"; IL: Insubric Line; Kn: Knorren mélange; Lo: Lostallo window; MC: Mesozoic cover of the Suretta and Tambo nappes; MG: Mesozoic cover of the Gotthard "massif"; NB: Axial trace of the Niemet-Beverin fold; TM: Turba mylonite zone; ZB: Bellinzona-Dascio zone. *AC*: Alp de Confin; *AlA*: Alpe Arami; *AT*: Alp de Trescolmen; *CG*: Cima di Gagnone; *Eh*: Einshorn; *MD*: Monte Duria; *Me*: Mesocco; *PF*: Passo della Forcola; *SB*: San Bernardino. Rectangle: Study area.

nappe and the overlying Tambo nappe (Figs. 3, 4). The structures of all these units were investigated in order to compare and, if possible, correlate different stages of deformation which have been defined by previous authors who mainly focussed either upon the Adula nappe or the overlying units (LÖW 1987, MARQUER 1991, MEYRE and PUSCHNIG 1993, SCHREURS 1993, MAYERAT DEMARNE 1994, PARTZSCH 1998).

As a result, four phases of ductile deformation were recognized within each unit; a first deformation phase of the Adula nappe can only be inferred mediately (see below). They are referred to as D1 to D5 for the Adula nappe and, to avoid confusion, F1 to F4 in the case of the overlying units. All of them, except D1 and D2 of the Adula nappe, are ascribed to postcollisional nappe stacking and further shortening whereas features related to the subduction stage are hardly preserved. Two processes mainly controlled the development of the present nappe stack: First, a strong top-north shearing which is dominant throughout the whole area and led to nappe stacking, and second, a top-east shearing which is distinctly discernible in the Tambo nappe and upper parts of the Misox zone but continuously fades towards the Adula nappe where it could only be detected by means of textural studies of quartz. In combination with this top-east shearing, south-vergent backfolds of all scales developed in front of the Tambo nappe.

2. Overview of the regional geology

The described units are part of the eastern flank of the Lepontine structural dome and therefore dipping towards the east with average angles around 30°. Hence, in the field the sequence of Eastern Swiss Penninic basement nappes,

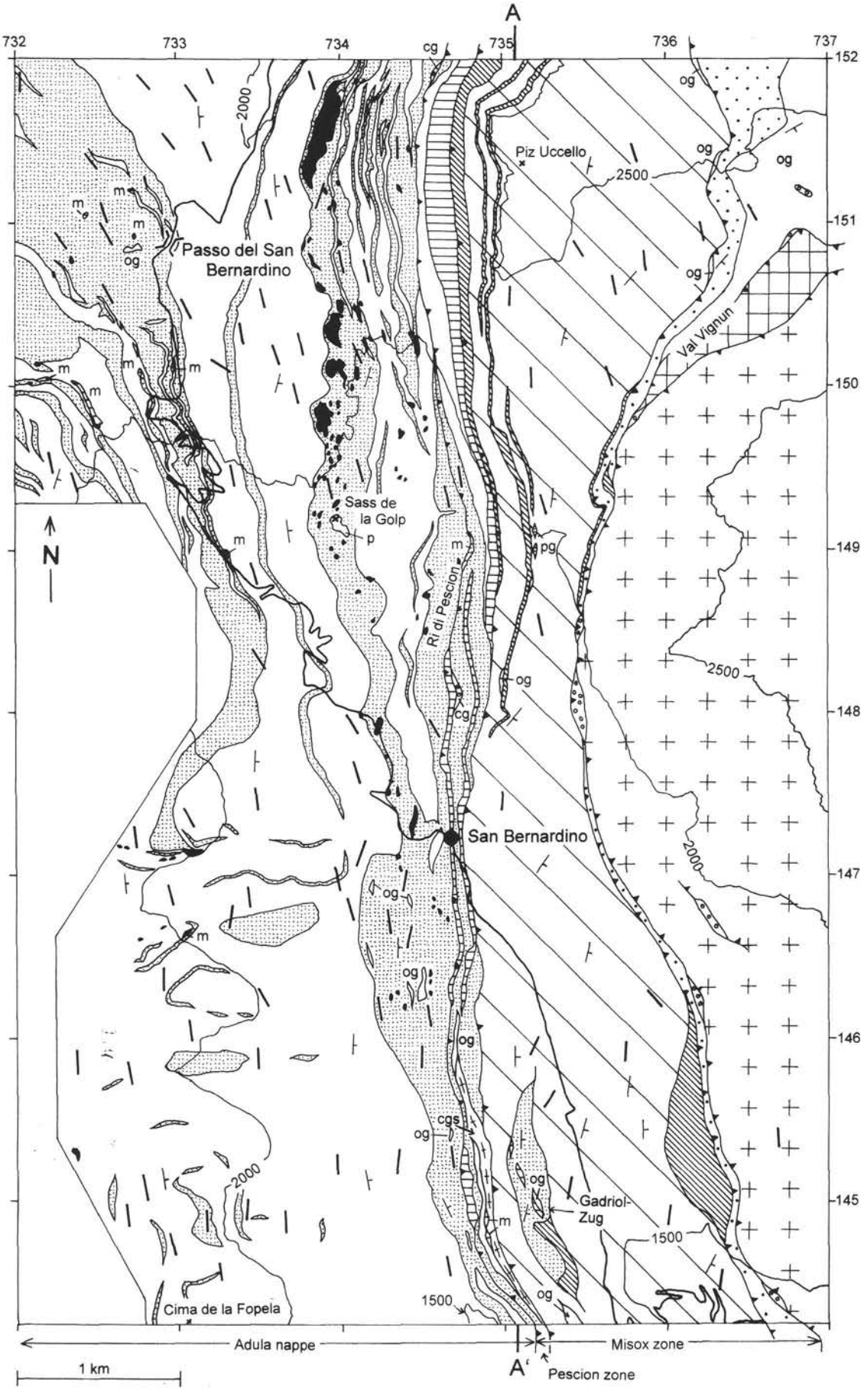
A
A'
732
733
734
735
736
737
152
151
150
149
148
147
146
145
cg
2000
2500
1500
og
m
pg
p
Piz Uccello
Passo del San Bernardino
Sass de la Golp
Ri di Pescion
Val Vignun
San Bernardino
Gadriol-Zug
Cima de la Fopela
N
Adula nappe
Misox zone
Pescion zone
1 km

comprising from bottom to top the Lucomagno-Leventina, Simano, Adula, Tambo and Suretta nappes, is exposed from west to east. To the north they are enveloped by North Penninic Bündnerschiefer which are rooted to the south in the Misox zone and, in the case of the Tambo and Suretta nappes, by the Schams nappes. To the south, these Penninic nappes are limited by a mylonitic steep belt associated with the Insubric line and to the southeast by the Bergell intrusion (Fig. 2).

Following the generally accepted statement that during Tertiary Alpine orogeny the Penninic nappes were subducted in southward direction, the reconstruction of the situation before the onset of continental convergence yields the sequence of the present nappe stack, seen from bottom to top, arranged from external (northern) to internal (southern) positions. With respect to the Valais ocean, time brackets for the continental break-up and the beginning of imbrication are inferred from the onset of sedimentation on oceanic basement in the Early Cretaceous (FLORINETH and FROITZHEIM 1994) and the age of the youngest sediments, respectively, which is late Paleocene to Early Eocene within the Arblatsch flysch (ZIEGLER 1956, EIERMANN 1988).

The Misox zone comprises all sedimentary units between the Adula and the Tambo nappe including incorporated cristalline slices (GANSSER 1937). At the boundary to the Adula nappe, a mixed zone of gneiss, marble, cargneule, amphibolite and greenschist occurs (Pescion zone, Figs. 3, 4; termed "Adulatrias" by GANSSER 1937). The lower and the upper Uccello zones, overlying the Pescion zone, represent the sediments of the Valais ocean and its ophiolites. They mainly consist of several types of impure marble and calcschist (Bündnerschiefer). Only the lower Uccello zone is rich in basic rocks. In the study area these are greenschists; from the village Mesocco to the south they are replaced by amphibolite facies rocks (TEUTSCH 1982). Metagabbros are reported from the northern lower Uccello zone by GANSSER (1937). Lenses of paragneiss, orthogneiss and marble collectively referred to as "Gadriolzug" (Figs. 3, 4; GANSSER 1937) are intercalated with these Bündnerschiefer and separate the lower from the upper Uccello zone. According to STEINMANN (1994), the lower Uccello zone continues northward into the Aul Schuppenzone, and the Upper Uccello zone becomes the Tomül nappe. The Grava nappe, the most voluminous of the Bündnerschiefer nappes farther north, wedges out into the Gadriolzug towards our study area. In addition, three smaller units accompany the front of the Tambo nappe: The Areua slice, probably originating from the Briançonnais basement; the Schams nappes, also of Briançonnais origin, which occupy larger areas northeast of the study area and envelop the front of the Suretta and Tambo nappes; and a mélange of unknown origin, the Knorren mélange (GANSSER 1937, MAYERAT DEMARNE 1994; Figs. 2, 3). The Areua slice is present in the study area as thin lenses of orthogneiss at the base of the Schams unit and as a thicker orthogneiss layer at the top of the same unit (Figs. 3, 4).

The protoliths of the Adula nappe, paragneisses, metapelites and Late Variscan granitoids (JÄGER et al. 1967, HÄNNY et al. 1975) were situated at the European distal margin (SCHMID et al. 1990). Due to imbrication during subduction, marbles and Bündnerschiefer of strong affinity with the Misox zone were incorporated as thin layers into the Adula nappe (VAN DER PLAS 1959, EGLI 1966, Figs. 2, 3, 4).

The Tambo nappe is derived from the Briançonnais continental domain which separated the Valais ocean from the Piemont-Liguria ocean. It is dominantly composed of paragneisses which already suffered Variscan deformation and to a minor extent of Late Variscan laccolithic granitoid complexes (MARQUER 1991, MAYERAT DEMARNE 1994). SCHMID et al. (1997, a,b) reconstruct the paleogeographic setting and structural evolution of the tectonic units comprised in the study area. This reconstruction is generally in line with our results, the only exception being the contemporaneity, assumed by SCHMID et al., of the Zapport deformation phase in the Adula nappe with the Niemet-Beverin phase in the Tambo, Suretta and Schams nappes (see below).

← Fig. 3
Geological map of the study area.

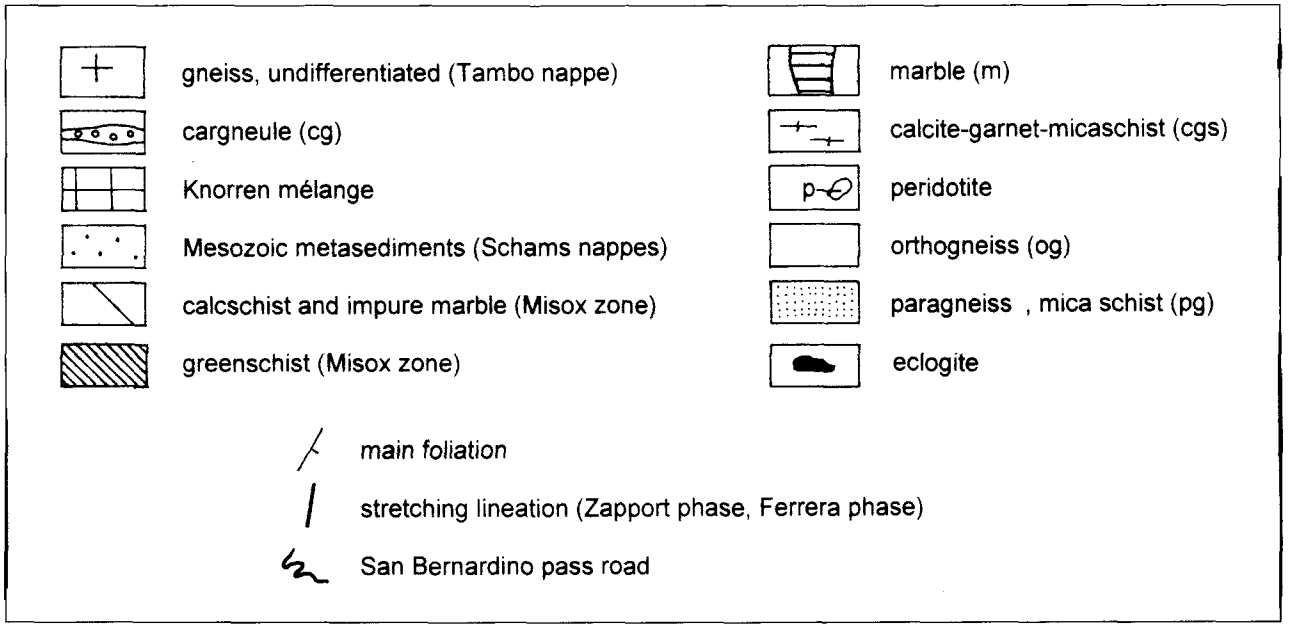

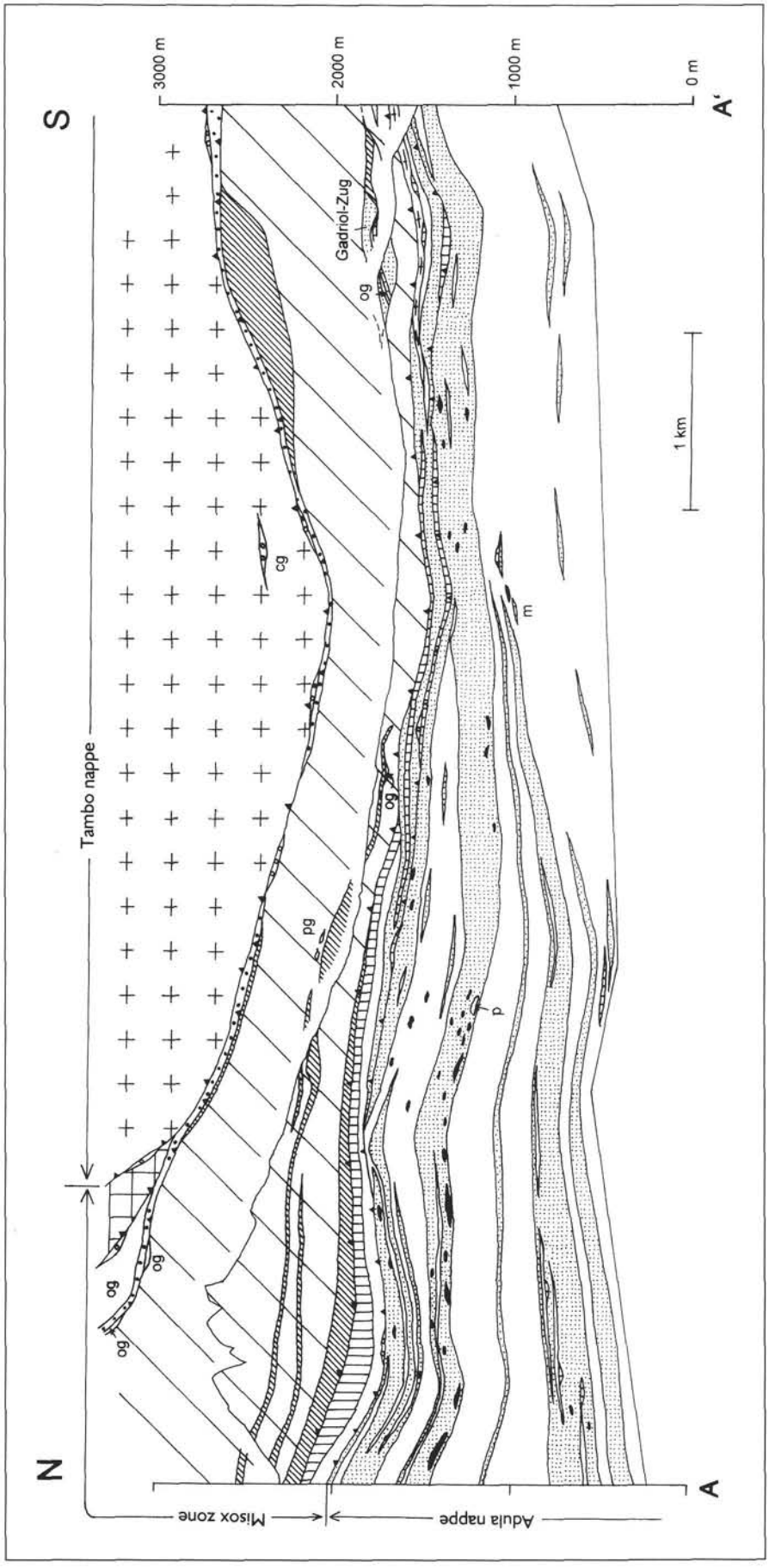

Fig. 4
Geological cross-section of the study area along *Swiss map* coordinate 735070 (trace of cross-section in Fig. 3).

Fig. 5
Deformation structures from the Adula nappe.
a) Layer of Mesozoic marble sliced into the Adula nappe during D1. Hammer is at the boundary between marble and overlying orthogneiss. Internal imbrication of dolomitic and calcitic layers was formed during the Zapport phase (D3) and indicates top-NNW (sinistral in this view) shear sense. Coordinates 732440/149930, view towards east-northeast.
b) D2 deformation: Thin section of an eclogite (sample R56; Swiss coordinates 733920/149815) containing mainly garnet (polygonal grains with dark outline) and omphacite. Trescolmen-phase (D2) foliation and lineation are horizontal in the picture. Horizontal white layer in the middle is quartz. The omphacite grains are elongated within the lineation. Note that inclusion-rich garnet cores are round whereas inclusion-free garnet rims are elongate, indicating that the garnet shape fabric formed by preferential growth. Green hornblende (dark) has grown from a late brittle fracture steeply inclined to the right. Scale bar is 500 μm; plane polarized light. Omphacite texture of this sample is shown in Fig. 7.
c) D2 deformation: Thin section of an eclogite (sample R54; Swiss coordinates 733920/149815) containing garnet, omphacite, and eclogite-facies barroisitic hornblende (elongate, poikilitic grain between the two arrows). Foliation and stretching lineation horizontal. As in Fig. 5b, green hornblende (dark) has grown from a late brittle fracture steeply inclined to the right. Scale bar is 500 μm; plane polarized light. Omphacite texture of this sample is shown in Fig. 7.
d) D3 deformation: Orthogneiss mylonite from the Adula nappe. Asymmetric K-feldspar porphyroclast indicates sinistral (top-N) shearing. Swiss coordinates 734710/146080.
e) D3 deformation: Isoclinal fold of the Zapport phase in orthogneiss. Swiss coordinates 732250/149740. NE is to the right, fold axis orientation is 161/05, outcrop is about 1 m high.
f) D5 deformation: South-vergent kink fold of the Carassino phase in orthogneiss. N is to the left. Swiss coordinates 732870/151570.

a)

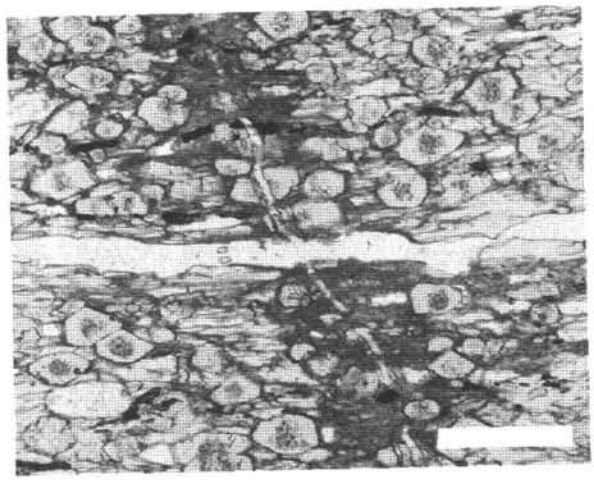

b)

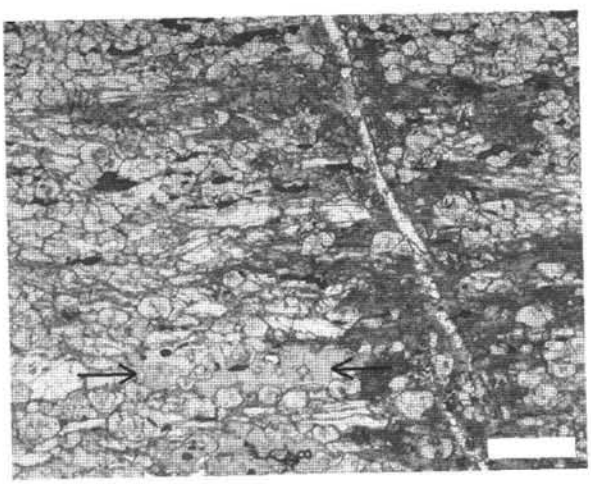

c)

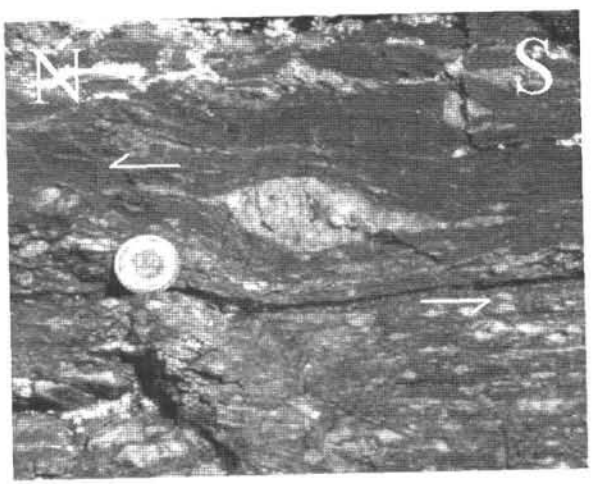

d)

e)

f)

3. Structural analysis of the Adula nappe

3.1 Overview

Recent studies on the structural evolution of the Adula nappe have been carried out by Löw (1987) for the north, Partzsch (1998) for the middle and Nagel (2000) for the south of the nappe. Whereas intense polyphase folding can be observed in the northern and southern parts, apart from a late undulation the main features of the middle Adula nappe are mylonitic foliations and lineations. They are only locally affected by folding which, however, in most cases allows to recognize clear overprinting relations and to classify the deformation phases D2, D3, and D4 according to the nomenclature bestowed upon them by Löw (1987) and Meyre and Puschnig (1993).

The present geometry of the nappe is one of a forward-dipping duplex (see Boyer and Elliott 1982) with layers of mostly para- and orthogneiss alternating at different scales. The majority of eclogite and amphibolite lenses appears aligned within distinct layers of paragneiss or metapelite which themselves alternate with orthogneiss at different scales (Figs. 3, 4). In addition, a lens of olivine-rich peridotite occurs at Sass de la Golp in the main eclogite-bearing layer (Fig. 3).

Whereas the northern and middle parts of the nappe occupy a coherent area, the situation along the southern steep belt is more complex. To the southwest the Adula unit continues into the Cima Lunga unit, framing the southern part of the underlying Simano nappe. To the southeast the Gruf unit is attached to the Adula nappe. The Gruf unit itself is limited to the north and south by the Tambo nappe and the Bergell pluton, respectively. The existence of the Lostallo window (Fig. 2; Künding 1926) in the central southern part of the Adula nappe, exposing rocks of the Simano nappe, has not been generally accepted (e. g. Spicher 1980) but recently Nagel (2000) and Nagel et al. (in press) presented convincing structural evidence for this window.

3.2 D1/Sorreda Phase

This first deformation stage can only indirectly be inferred from the presence of impure marbles and Bündnerschiefer, locally accompanied by basic rocks, deep within the Adula nappe. They are always in tectonic contact with the gneissic rocks of the Adula nappe and possess strong lithologic affinities with the Mesozoic rocks of the Misox zone (Fig. 5a; van der Plas 1959, Egli 1966). Therefore, a first imbrication of alpine age must be inferred. Although most of the slivers of this "Internal Mesozoic" occupy distinct structural levels, it seems doubtful if tracing these levels over larger areas would visualize the D1 structure, because of later D3 imbrication. Possibly the high-frequency layering of para- and orthogneisses is due to the twofold imbrication. A D1-foliation as recorded by Löw (1987) cannot be confirmed in our study area, but curved and planar internal foliations of garnet porphyroclasts observed in thin-sections are assumed to be relics of D1.

3.3 D2/Trescolmen Phase

The eclogite lenses in the study area have roughly ellipsoidal shapes (between prolate and "plane strain") with the long axis parallel to the D3 lineation in the surrounding rocks. Fish-mouth structures occasionally found at the terminations of eclogite lenses indicate that they were indeed formed by boudinage. Eclogite lenses contain D2 foliations and lineations that are unconformable with the D3 main foliation and stretching lineation of the surrounding rocks. The D3 main foliation in the surrounding rocks dips east at an average of 29° (Fig. 6b), and the D3 lineation is north-northwest-south-southeast (see below; Fig 6c). In contrast, the foliation of the mafic lenses, including eclogite and variably amphibolitized eclogite, shows a larger spread (Fig. 6a). The pole figure shows foliations that are parallel to D3 of the surrounding rocks, but also aberrant orientations, most of them steeply dipping east. The latter are found in the least retrograded boudins, whereas the former occur in the amphibolitized eclogite. A similar situation applies to the lineations (Fig. 6a). Lineations in the least overprinted eclogites are east-west and curve towards north-south with increasing degree of amphibolitization. Hence, the D2 structures corresponding to deformation under eclogite facies conditions are (almost) exclusively preserved within the comparatively rigid eclogitic cores of larger mafic bodies. At their amphibolitic rims and within the other rocks of the Adula nappe, D2 structures are completely extinguished by the strong amphibolite-facies D3 mylonitization. Meyre and Puschnig (1993) introduced the term "Trescolmen phase" for isoclinal folds within eclogite boudins at the locality Trescolmen. Later Partzsch (1998) extended the term to all eclogite-facies structures in the Adula nappe. We follow this terminology.

The eclogites consist of garnet, omphacite, rutile, quartz, and paragonite (see also Meyre et al. 1997). Additionally, a barroisitic hornblende occurs in several of the eclogites. This amphibole formed under retrograde, but still eclogite-facies conditions (Fig. 5c; Hundenborn 2001). The rocks have mostly well-developed foliation and lineation. The stronger the foliation and lineation, the finer is the grain size of omphacite and garnet. Hence, deformation was associated with grain-size reduction. Foliation and lineation are in thin section defined by aligned omphacite, slightly elongate, hypidiomorphic garnet grains, and by alternation of

Fig. 6 →
Lower hemisphere Schmidt projection plots of structural elements in the study area.
a) Poles to foliation (squares) and stretching lineation (circles) in basic rocks of the Adula nappe, formed during the Trescolmen (D2) and Zapport (D3) phases.
b) Poles to foliation of the Zapport phase in the Adula nappe, except for basic rocks. Maximum is located at 94/29.
c) Stretching lineation of the Zapport phase in the Adula nappe, except for basic rocks. Maximum is located at 166/10.
d) Poles to fold axial planes (squares) and fold axes (circles; maximum: 68/24) of the Leis phase (D4) in the Adula nappe.
e) Poles to fold axial planes (squares) and fold axes (circles) of the Carassino phase in the Adula nappe.
f) Poles to Ferrera phase (F1) foliation in the Misox zone and Tambo nappe (maximum at 105/33).
g) Ferrera phase (F1) stretching lineation in the Misox zone and Tambo nappe (maximum at 177/16).
h) Poles to Niemet-Beverin phase (F2) fold axial planes (squares; maximum 40/35) and fold axes (circles; maximum 72/27) in the Misox zone and Tambo nappe.
i) Niemet-Beverin phase (F2) stretching lineation (maximum 68/20) in the Misox zone and Tambo nappe.
j) Poles to Domleschg phase (F3) fold axial planes (squares) and fold axes (circles) in the Misox zone and Tambo nappe.

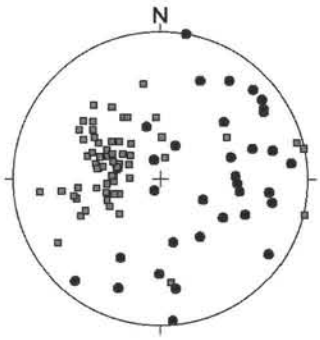

a) D2 and D3 structures in basic rocks

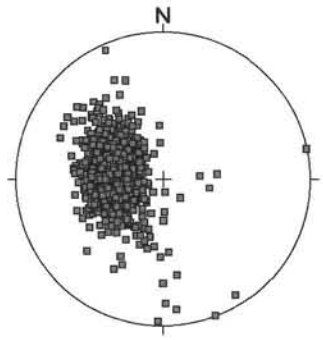

b) D3 foliation in all other rocks

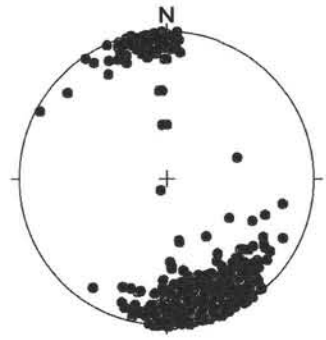

c) D3 stretching lineation in all other rocks

Structural elements of the Adula nappe

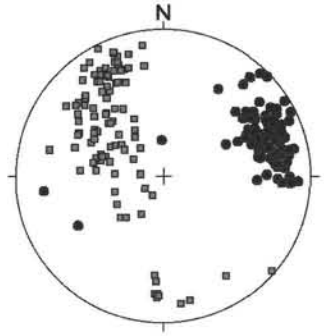

d) D4 fold axes (dots) and fold axial planes (squares)

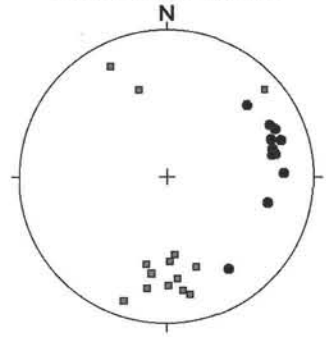

e) D5 fold axes (dots) and fold axial planes (squares)

Structural elements of the Misox zone and the Tambo nappe

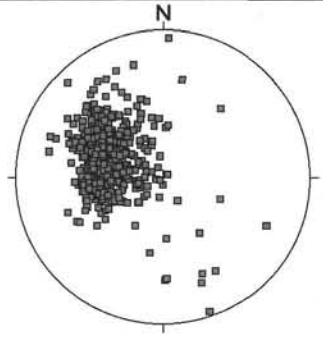

f) F1 foliation

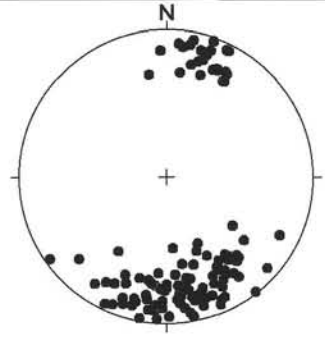

g) F1 stretching lineation

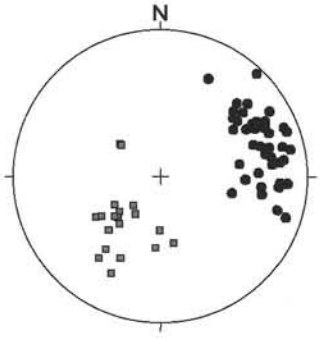

h) F2 fold axes (dots) and fold axial planes (squares)

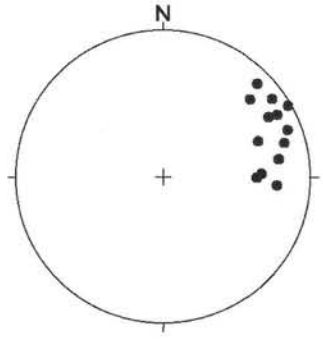

i) F2 stretching lineation

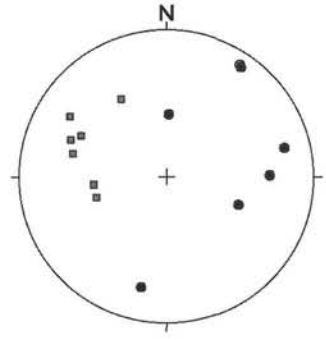

j) F3 fold axes (dots) and fold axial planes (squares)

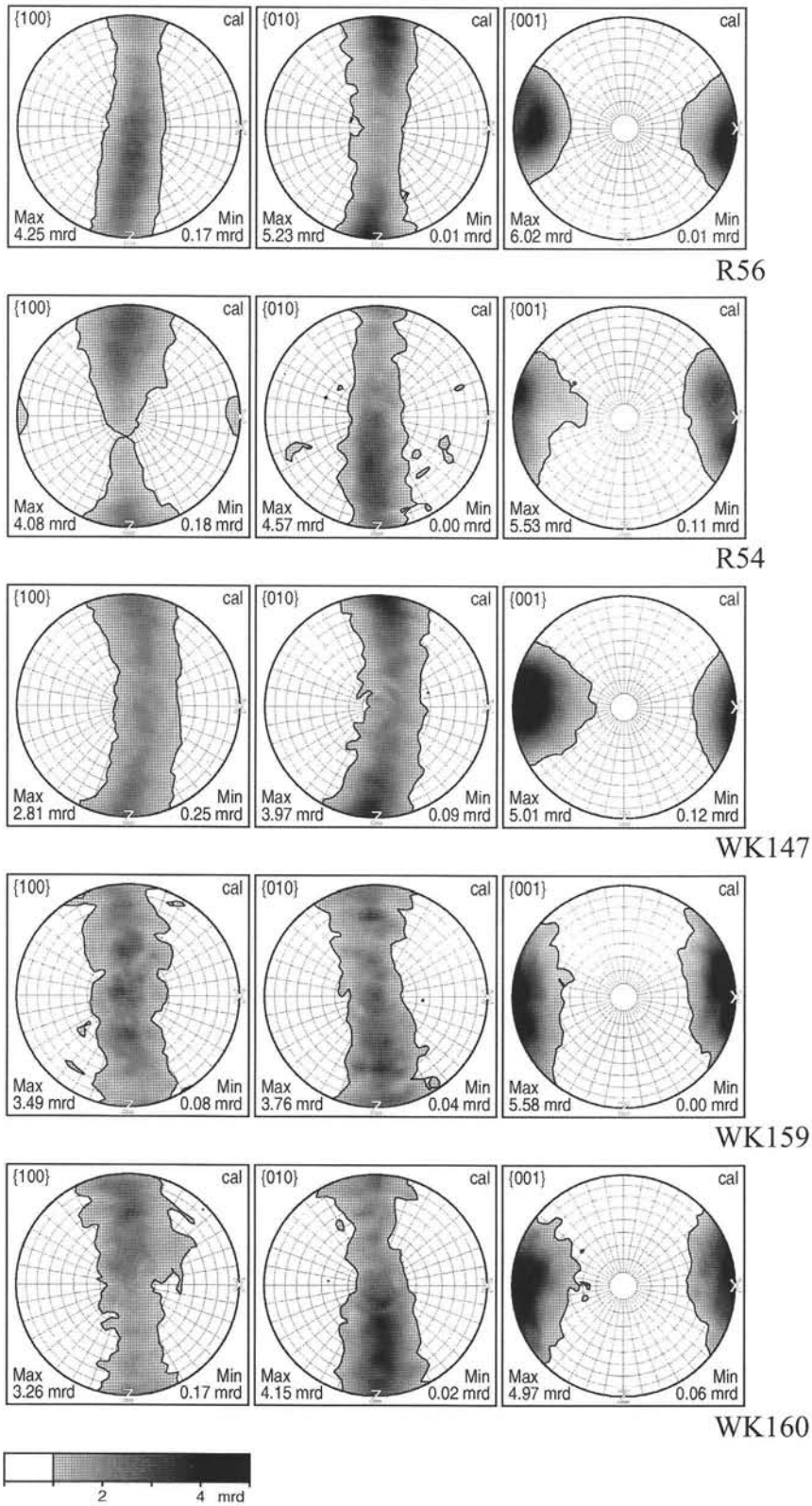

Fig. 7
Texture of omphacite in deformed eclogites obtained from neutron diffraction. Upper hemisphere, equal-area projection. Pole figures were calculated from the orienation distribution function obtained from seven reflections in four clusters. Trace of the foliation and lineation (x direction) is horizontal east-west in the pole figures, y direction is at the centre, and z direction is north-south. Sample locations of R56 and R54: see caption of Fig. 5. WK147 is from Alp de Confin (731 100/146 010), WK159 and WK160 are from I Corn de Golin near Capanna Buffalora (732 625/134 775). For further explanation see text.

garnet-rich and omphacite-rich layers. The garnet grains have a round, inclusion-rich core and an inclusion-free rim. The rim is relatively thick in the direction of the lineation, and thinner elsewhere. This suggests that the core grew before the deformation that produced the microstructure, and the rim grew synkinematically and preferentially in the lineation direction, leading to the elongate shape (Fig. 5b). The eclogite-facies amphiboles form large (up to 0.5 cm), elongate, poikilitic grains. In most cases, they are aligned parallel to the D2 lineation. For these, we assume that they grew during D2. In some places, however, the high-pressure amphibole is randomly oriented and has grown across lineation and foliation. There, the amphibole has grown after D2 deformation stopped. We conclude that the D2 deformation which produced the foliation and lineation ended when the rocks were still under eclogite-facies conditions. Green, amphibolite-facies amphibole overgrows the eclogite paragenesis along brittle fractures cutting the foliation (Fig. 5b, c).

Neutron texture studies have been carried out on two samples of eclogite from the study area (R56 and R54, Swiss coordinates 733 895/149 920 and 733 920/149 815, respectively), and, additionally, on three eclogite samples from the Adula nappe outside the study area (WK147, WK159, and WK160). The measurements were done on the texture diffractometer SV7-b at the reactor FRJ-2 at Forschungszentrum Jülich (JANSEN et al. 2000). Since the recorded neutron diagrams showed strongly overlapped Bragg reflections of various mineral phases, the BEARTEX programme system (WENK et al. 1998) was employed to calculate 3-dimensional orientation distributions from the experimental observation and to obtain pole figures also for non-observed reflections.

In the case of R56, without eclogite-facies amphibole, the {010} pole figure of omphacite shows a girdle distribution on a great circle perpendicular to the stretching lineation, with a maximum perpendicular to the foliation (Fig. 7). The {100} pole figure reveals a girdle distribution as well, with a maximum in the y-direction. Consequently, the {001} poles are concentrated close to the x-direction. On close inspection, however, they

form two submaxima within the foliation plane and a small distance away from the x-direction, in accordance with the omphacite β angle of 106.85°. The girdle distributions of the {100} poles and b-axes, although they are not even, indicate strain lying within the field of constriction.

The omphacite texture in R54, an eclogite containing high-pressure amphibole, resembles the one of R56 with the only difference that it appears rotated by 90° around the x-axis of the strain (Fig. 7). The {100} and {010} maxima are located close to z and y, respectively, and the two {001} submaxima are at a small distance from x in the x-z plane.

Three more omphacite textures were measured on samples from the Adula nappe outside the study area. WK147 is from a large eclogite boudin at Alp de Confin, less than one km west of our study area. This boudin was described in detail by PARTZSCH (1998). There the foliation is steep and strikes east-west, and the stretching lineation dips shallowly east. WK159 and WK160 are from I Corn de Golin near Capanna Buffalora, 9.5 km south of our study area. The textures of all three samples are very similar to the ones of R56 and R54. WK159 is an extreme L type (HELMSTAEDT et al. 1972), where {010} is evenly distributed on a great circle. In WK147, the {010} maximum on the great circle is perpendicular to the foliation, as in R56, and in WK160, it is oblique to the foliation.

It can be stated that all samples measured so far from the Adula nappe correspond to the L type of HELMSTAEDT et al. (1972), suggesting constrictional deformation (GODARD and VAN ROERMUND 1995). Since this texture is observed in eclogites with and without the retrograde high-pressure amphibole, we assume that the constrictional deformation lasted from the pressure peak to the the earliest stage of exhumation.

The fact that the eclogite and amphibolite boudins are elongate in the direction of the D3 lineation (i. e. north-northwest-south-southeast; see also MEYRE and PUSCHNIG 1993) suggests that the boudins were rotated before or during D3. Under this assumption, the east-west trend of the lineation in the least retrograded eclogite lenses would not represent the original configuration. A possible scenario of shearing and later boudinage of the eclogites is given in PARTZSCH (1998). He assumes that the stretching direction during the Trescolmen phase was north-south. This is reasonable but has not yet been corroborated by direct evidence.

The structural evolution of the eclogites can be summarized as follows: Under peak pressure and during beginning exhumation, more or less coherent basic layers were deformed by constrictional coaxial shearing (D2). The deformation undergone by the gneissic country-rocks at that time is not preserved because of a strong D3 overprint. Additionally, the generation of isoclinal folds within the boudins (MEYRE and PUSCHNIG 1993) was probably associated with D2. The boudinage occurred between D2 and D3 or during D3. Also during D3, the boudins were rotated and reoriented with their long axes parallel to the D3 stretching lineation. Simultaneously, the outer parts of the boudins were re-equilibrated under D3 amphibolite facies conditions. The amphibolitic rims of the boudins were almost completely overprinted by the D3 foliation and stretching lineation; only the eclogitic cores of the boudins behaved rigid as indicated by the brittle fractures along which green hornblende has grown (Fig. 5b, c).

3.4 D3/Zapport Phase

The penetrative D3 foliation and D3 stretching lineation are by far the dominant structures of the middle Adula nappe. They are only absent in eclogitic cores of mafic boudins. At least at the scale of a single outcrop the mylonitic foliation is parallel to the layering which is mostly the alternation of para- and orthogneisses, except in the hinges of D3 folds (see below). From the map and more obviously from the cross section (Fig. 4) it becomes visible that individual layers can be followed into higher positions with respect to the nappe's roof going from north to south. This observation, already made by JENNY et al. (1923), is valid for the whole Adula nappe and constitutes its geometry of a forward-dipping duplex (see BOYER and ELLIOTT 1982). On an average, foliation and layering strike north-south and dip towards the east (94°) around 29° (Fig. 6b). Deflections from this orientation result from late D5 undulations. In most cases the D3 stretching lineation is formed by aligned aggregates of quartz or quartz and feldspar. Therefore, it is always more strongly developed in orthogneisses than in paragneisses. The trend of the lineation is north-south to northwest-southeast (Fig. 6c; maximum 166/10). Shear sense indicators such as asymmetric porphyroclasts in K-feldspar augengneisses (Fig. 5d) and C'-type shear bands in paragneisses and metapelites unambiguously prove top-north-northwest directed shear movements during D3.

Apart from C'-type shear bands which are locally abundant enough to make up an extensional crenulation, D3-related folds are very rare. Only small-scale tight to isoclinal folds with amplitudes of cm- to dm-dimensions could be observed (Fig. 5e). Their axial planes are always parallel to the D3 foliation, the compositional layering is folded. The D3 fold axes are parallel or subparallel to the D3 lineation. The vergence is variable but no superordinate pattern can be recognized by its distribution. This supports the impression that D3 folding is only related to local deflections of the apparently almost homogeneous overall strain and does not have much imprint on the geometry of the middle Adula nappe.

Neutron texture studies on quartz are consistent with the results of fieldwork and, additionally, indicate overprinting of the Zapport phase mylonite by minor, top-east to -northeast directed shearing at a later stage (PLEUGER et al., 2002). Two paragneissic samples from the Adula nappe have been studied one of which shall be presented here. The other sample yielded similar results but has a weaker texture. Sample A48 comes from a quartz-rich (ca. 90%) paragneissic layer (Swiss coordinates 732 560/150 470) and contains additionally phengite, garnet, chlorite and some minor constituents. The phengite- and chlorite-{001} pole figures (Figs. 8c, d) reflect the fact that tabular grains of these minerals define the foliation. The slight asymmetry of the chlorite {001} maximum is caused by the fact that some of the chlorite is aligned in shear bands dipping shallowly to the left. Quartz is dynamically recrystallized, mainly by subgrain rotation, to a grain size of about 100 to 500 μm. The c-axis pole figure of quartz (Fig. 8e) yields a girdle distribution steeply inclined to the right (eastsoutheast) and indicates a sinistral, top-north-northwest directed sense of shear. A strong single maximum, situated between the centre and the periphery of the pole figure, is superposed on the girdle. Around this maximum discrete maxima of the

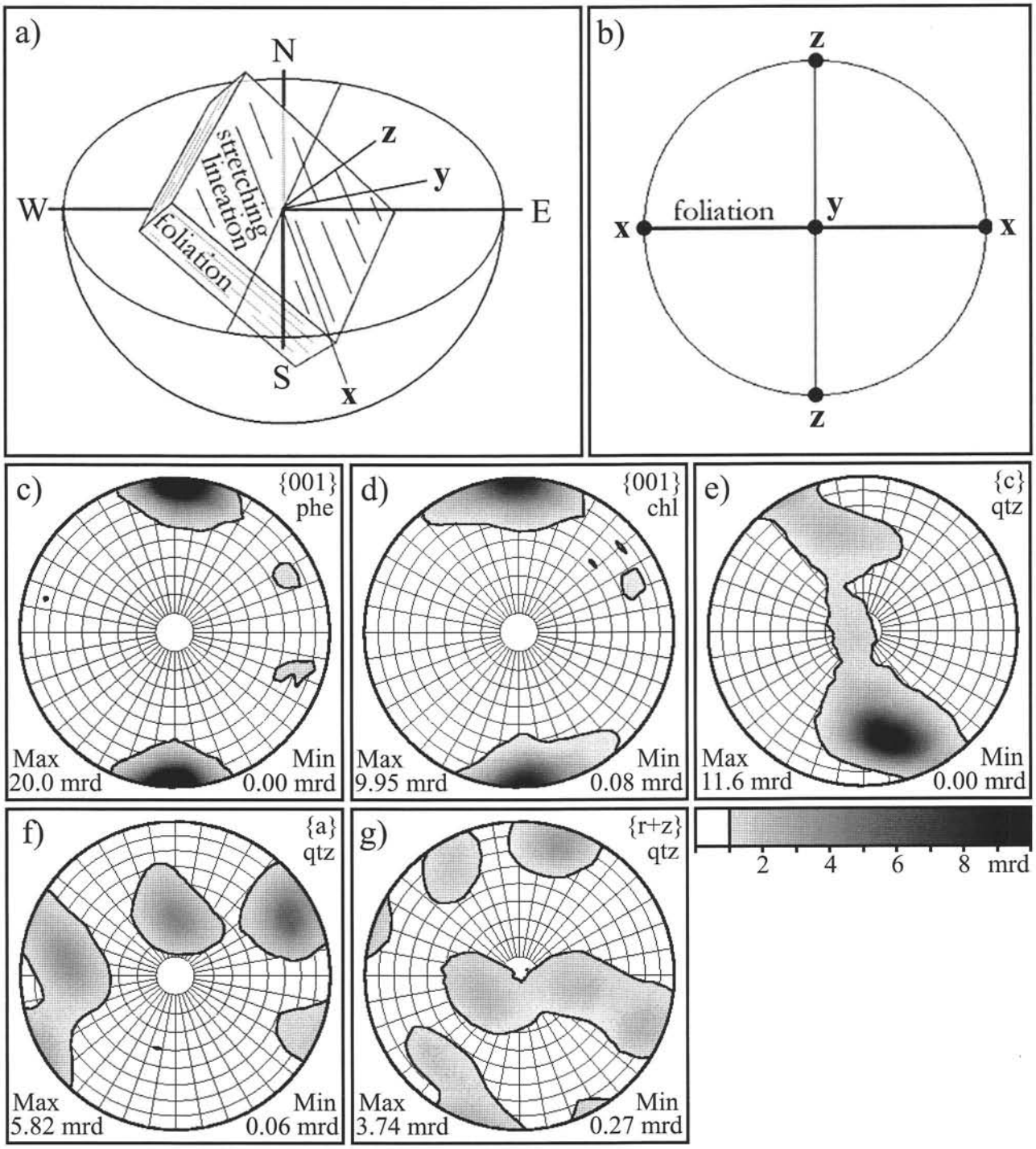

Fig. 8
Texture of quartz, phengite, and chlorite from sample A48, a paragneiss from the Adula nappe. Upper hemisphere, equal area projection. Phengite and chlorite pole figures result from averaging higher-order reflections of the (001) plane, quartz pole figures were calculated from the orientation distribution function derived from the 100, 101/011, 110, and 111 reflections.
a) Schematic representation of sample orientation and strain x-, y-, and z directions in geographic coordinates.
b) Orientations of principal strain axes (x, y, z) and the trace of the foliation in the pole figures.
c) Pole figure of the phengite {001} pinacoid with maximum at the pole of the foliation plane.
d) Pole figure of the chlorite {001} pinacoid with maximum at the pole of the foliation plane.
e) Pole figure of the quartz c-axes, indicating sinistral, top-N shearing.
f) Pole figure of quartz {a} prism, showing the orientation distribution of the a axes.
g) Pole figure of the superposition of positive and negative rhombohedra {r+z} of quartz.

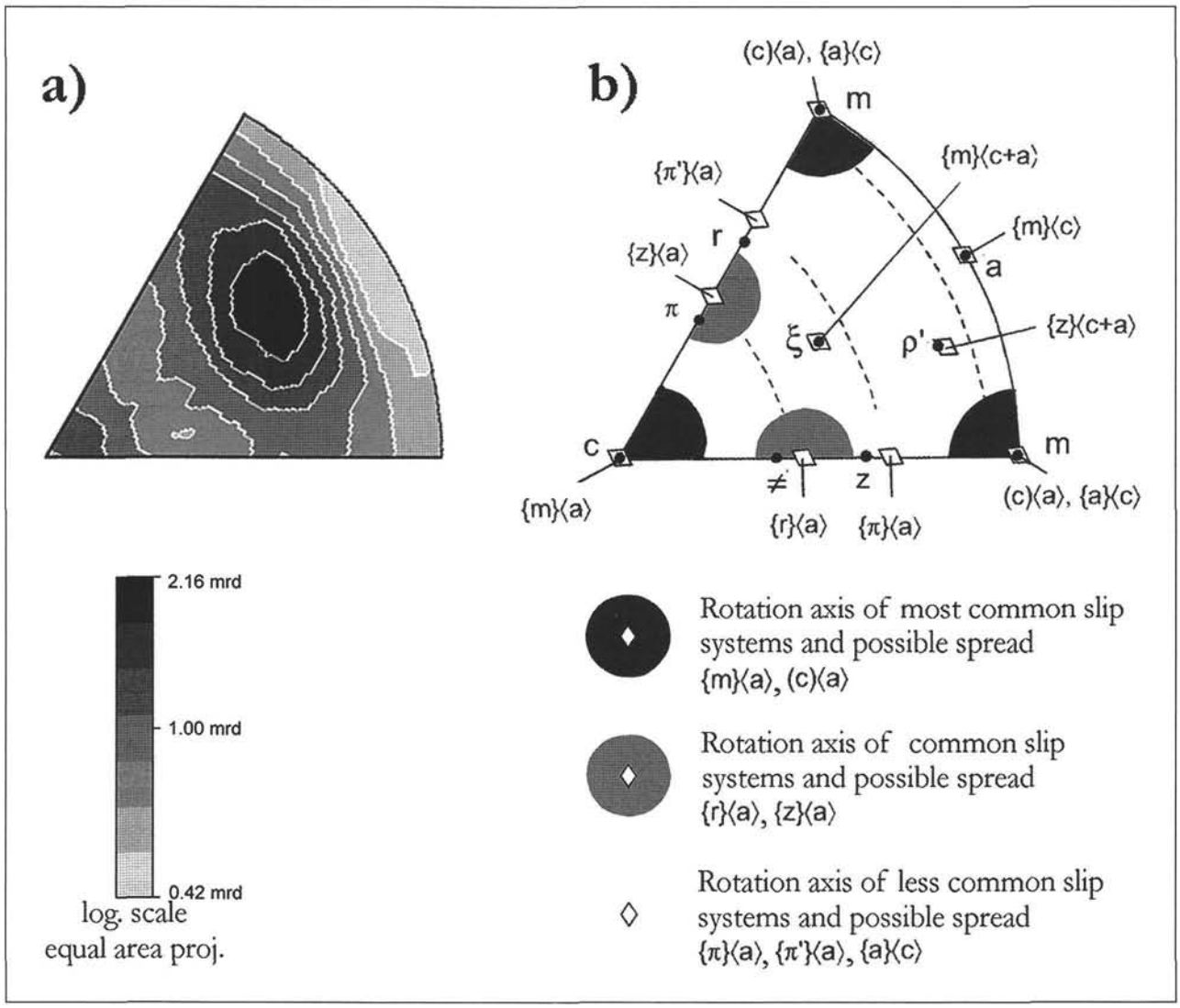

Fig. 9
a) Inverse pole figure of quartz in sample A48 (paragneiss from the Adula nappe) as calculated from the orientation distribution function, showing the orientation density of the y axis of strain in the framework of the crystallographic directions.
b) Orientations of some crystal directions and of the rotation axes of common quartz slip systems within the inverse pole figure (modified after NEUMANN 2000). Note that the maximum in (a) does not coincide with any of the positions predicted for common slip systems.

quartz-{a} and -{r+z} pole figures (Fig. 8f, g) occupy the great circle and small circles, respectively. As shown by the inverse pole figure (Fig. 9) the position of the c-axis maximum can neither be the result of basal <a> nor of rhomb <a> slip. Therefore, grain-shape analyses with SURFOR and PAROR methods (PANOZZO 1983, 1984) have additionally been carried out on an x-z section (Fig. 10a) and an y-z section (Fig. 10b) in order to find out whether the texture reflects an overprint by a second phase of deformation. The SURFOR-analysis of the x-z section (Fig. 11a) shows two maxima of grain boundary orientation distribution shallowly and steeply inclined to the right. The x-z PAROR-analysis (Fig. 11b), consequently showing one maximum inclined to the right, indicates a sinistral sense of shear, i. e. top-north-northwest. Both the SURFOR- and, more obviously, the PAROR-analyses of the y-z section (Fig. 11c, d) reveal single maxima inclined to the left which is southwest in geographic coordinates. These distributions substantiate a late top-northeast shear. Looking back at the quartz-c-axis pole figure, it appears most likely that the girdle distribution and the strong single maximum, caused by basal <a> slip, were formed during the north-northwest verging D3 movements (with the strong maximum originally located at the periphery of the pole figure) and later reoriented by more or less perpendicular, roughly east to northeast directed shear, corresponding to the Niemet-Beverin phase of the higher units (see below).

3.5 D4/Leis phase

From the northern Adula nappe, where Leis phase deformation led to a fold system with wavelengths of km-scale and a stretching lineation parallel to the east-northeast-trending fold axes (LÖW 1987), structures related to the Leis phase die away towards the upper middle Adula nappe. Only few folds in the study area can be ascribed to D4. They deform the D3 foliation and their geometry differs significantly from that of D5 folds. In accordance with BAUM-

GARTNER and LÖW (1983) two different types of Leis phase folds can be distinguished: First, recumbent tight, almost isoclinal folds one of whose limbs is often cut off parallel to the D3 foliation and, second, upright tight to open folds with fold axial planes almost perpendicular to the average D3 foliation. Apart from these two extremes, folds with an intermediate geometry appear quite frequently. All the D4 folds have wavelengths of some dm to m. In some cases a crenulation and an axial plane foliation are developed close to the fold hinges. The D4 fold axes dip moderately towards east-northeast (Fig. 6d); no D4 stretching lineation was observed.

Within orthogneiss folds of upright and intermediate geometry are often situated at the northern edges of quartzitic boudins. Although they may genetically differ from proper D4 folds because their formation should have been strongly influenced by the competence contrast between the boudins and their surroundings, these folds suggest that the abundant boudinage of quarzitic layers within orthogneiss probably took place during D4. If so, top-north movements within the Adula nappe were still active during the Leis phase because the boudins are sometimes displaced against each other along shear bands indicating that sense of movement. Furthermore, the fact that by far most D4 folds, especially the recumbent ones, are north-vergent, adds some weight to this view which is in line with results of PARTZSCH (1998) who proved Leis phase top-northwest movements for the lower part of the middle Adula nappe. However, within our study area, the Leis phase resembles a weaker and still diminishing continuation of the Zapport phase rather than an independent stage of deformation.

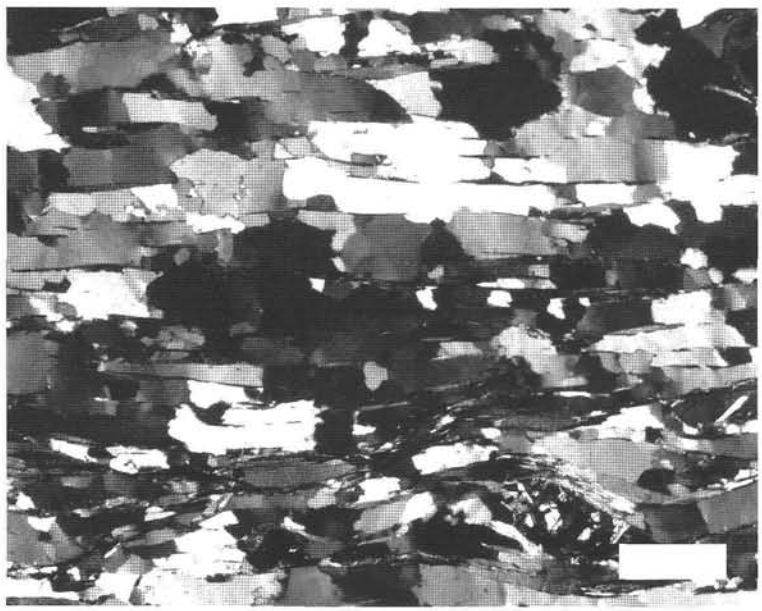

a)

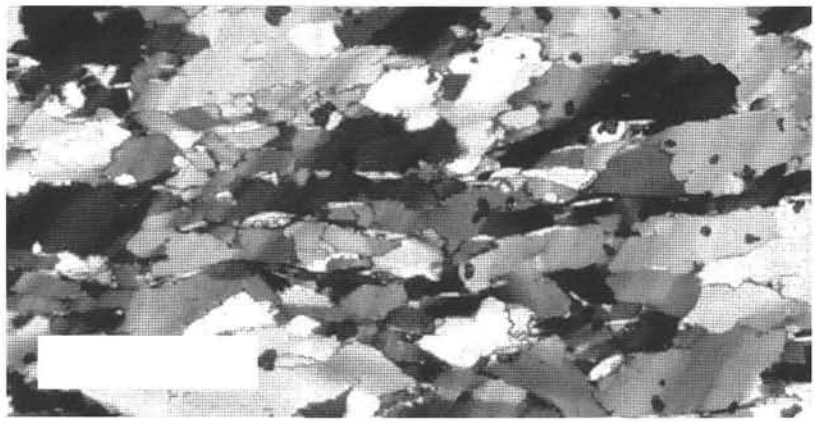

b)

Fig. 10
Thin section photographs of sample A48.
a) x-z section (parallel to stretching lineation, perpendicular to foliation). NNW is to the left. Sinistral (top-NNW) shear sense indicated by mica fish (lower right) and quartz grain boundary obliquity. Scale bar is 500 µm.
b) y-z section (perpendicular to stretching lineation and foliation) of the same sample. NE is to the right. Note deformation bands dipping to the left. Scale bar is 500 µm.

3.6 D5/Carassino phase

Within the studied area, an undulation and flexural folding are the latest ductile deformations. The intensity of undulation is not equal, but within some structural levels upright gentle folds with wavelenghts of some Dm and comparatively small amplitudes can be observed. From these structural levels the intensity of folding, which appears to be independent of the lithology, decreases upwards and downwards.

The D5 flexures are mostly south verging (Fig. 5f) and have fold axes plunging towards northeast to southeast (Fig. 6e). Along the short limbs of the antiforms layering and D3 foliation are lowered by an amount of some cm to dm. They are restricted to orthogneissic layers where they can be traced some Dm along the fold axes.

Late undulation and flexures within the middle Adula nappe have been attributed to the Carassino phase by MEYRE and PUSCHNIG (1993). The Carassino phase was defined by LÖW (1987)

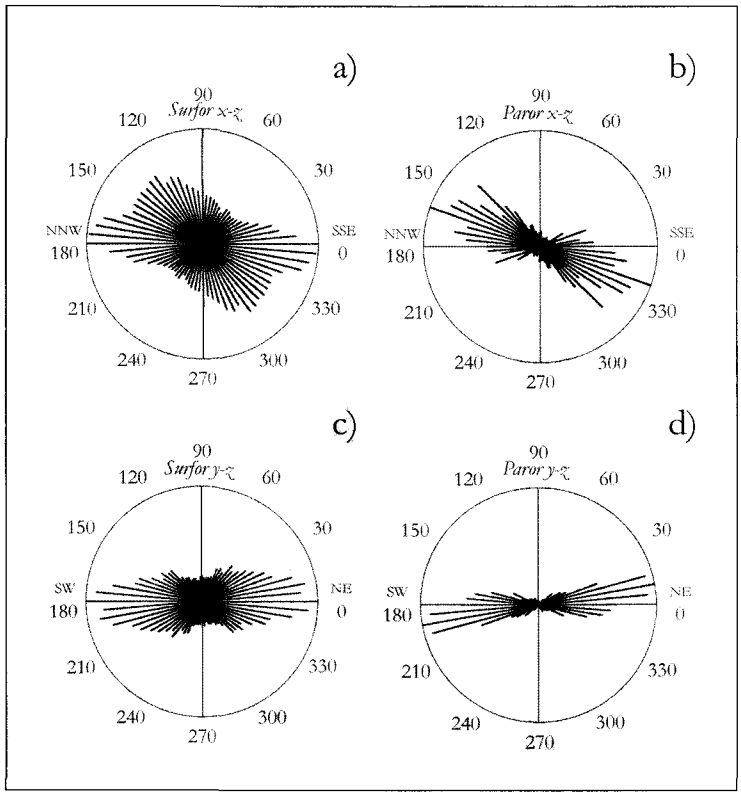

Fig.11
Rose diagrammes of orientation distributions (PANOZZO 1983, 1984) of recrystallized grain boundaries (SURFOR) and grain long axes (PAROR) in sample A48 (see Fig. 10).
a) SURFOR analysis of the x-z section;
b) PAROR analysis of the x-z section;
c) SURFOR analysis of the y-z section;
d) PAROR analysis of the y-z section.

for the northernmost part of the Adula nappe where it comprises a huge north verging flexure and its parasitic folds. As in the case of the Leis phase, Carassino-phase structures fade out towards the middle Adula nappe. The relative age of the undulation remains uncertain due to the lack of clear overprinting relations with D4. Geometric similarities of late, i.e. upright, D4 folds to the coaxial undulation suggest that the latter directly succeeded D4 or can even be reckoned among the D4 structures. Therefore, some uncertainties remain when the deformations described above are correlated with the Carassino phase.

4. Structural analysis of the Misox zone and the Tambo nappe

4.1 Overview

The deformation phases of the Tambo nappe and Misox zone will be discussed together since they yield the same set of structures and can unequivocally be correlated. This was already shown by MAYERAT DEMARNE (1994) who carried out structural work within the northernmost Tambo nappe and the units in front of it, hence a study area partly identical with ours. This and other works by BAUDIN et al. (1991, 1993) and MARQUER (1991) in the Tambo nappe and SCHREURS (1993, 1995) in the Schams nappes led to the recognition of a regionally consistent deformation history of the units above the Adula nappe. Therefore it is possible to correlate our deformation phases F1 to F4 with those defined and discussed by MILNES and SCHMUTZ (1978), PFIFFNER (1977), SCHREURS (1995), and SCHMID et al. (1997b).

Early work, especially precise mapping and description of the units between the Adula and the Tambo nappes, has been carried out by GANSSER (1937). The lowermost part of the Misox zone is marked by its gradual transition from the Adula nappe. Above a structural level characterized by the sporadic appearance of cargneule, thin slices of Bündnerschiefer, impure marble and greenschist appear between dominant Adula gneisses; the proportion of Adula gneisses decreases upward. Following GANSSER (1937), slivers of Adula gneisses do not occur above the first larger greenschist horizon which is therefore the upper boundary of what he calls "Adulatrias", referring to a characteristic, several m thick band of probably Triassic dolomite marble that is common to all complete outcrops of this unit. This term, however, is misleading in that the main character of the unit is that of a tectonic mélange whose rocks are mostly gneisses and Bündnerschiefer. Therefore we use the term Pescion zone since it is, within our study area, best exposed in the stream bed of Ri di Pescion (Fig. 3). Another excellent outcrop of this zone is above Tällialp (Swiss coordinates 734750/152050), 50 m north of our study area.

The Pescion zone is overlain by an alternation of some m to Dm thick layers of impure marble, Bündnerschiefer (i. e. more or less calcareous phyllites and micaschists with intercalations of impure marble), and greenschists being in tectonic contact with each other. From this lower Uccello zone the upper Uccello zone differs in containing only very few lenses of greenschist. Both zones are locally separated by incoherent slices of orthogneiss, paragneiss, serpentinite, and Triassic dolomite marble making up the "Gadriolzug" (GANSSER 1937; Fig. 3, 4). To the south the Misox zone can be followed into Val de la Forcola where it wedges out between the Adula and Tambo nappes at Passo della Forcola (Fig. 2). Further to the southeast the Adula and Tambo nappes are separated by the Miocene Forcola normal fault (MEYRE et al. 1999b). The Chiavenna ophiolite, situated between the Tambo nappe and the Gruf unit, again represents remnants of the Valais ocean (SCHMID et al. 1996).

Four more units of the Misox zone reach into the northeastern part of the study area (Val Vignun) structurally overlying the upper Uccello zone: Orthogneisses belong to the Areua slice which occupies two different structural levels separated by the westernmost offshoots of the metasedimentary Schams nappes. In the study area the Schams nappes lithologically resemble the lower and upper Uccello zones but can be distinguished by slivers of cargneule, white marble, and dolomitic breccia. Those rocks can be ascribed to the subunit 1b of the Gelbhorn unit in the sense of RÜCK (1995) by comparison of lithology. Between the upper level of the Areua slice and the Tambo nappe ap-

pears the Knorren mélange. It mainly consists of paragneiss, impure marble, quartzite and a gneissic breccia. Finally, slivers of cargneule occuring at the base of the Tambo nappe constitute the Andrana zone (STROHBACH 1965).

4.2 F1/Ferrera phase

The penetrative F1 foliation is the main foliation throughout the studied parts of the Misox zone. Its average orientation is 105/33 (Fig. 6f) but in front of the Tambo nappe, which does not reach as far north as the Adula nappe, it is bent into a northeast-southwest striking and steeper orientation due to the widening of the Misox zone. It runs parallel to the contacts of the units described above and their internal layering. An F1 stretching lineation plunges shallowly to the south (maximum 177/16, Fig. 6g). Locally even two lineations at small angles to each other can be discerned but no statement on their relation is possible. Stretching lineations are best developped within the marbles and gneissic rocks whereas in the phyllites they are difficult to distinguish from an F1 crenulation or absent. Within the upper part of the Misox zone, the lineation is sporadically extinguished by F2 overprint. Shear sense indicators related to this F1 stretching lineation are not as frequent as in the Adula nappe but unequivocally point to top-north shear movements as well. For these reasons F1 must be held responsible for nappe stacking of all the units described in chapter 4 and of the Tambo nappe where a mylonite horizon at its bottom yields the F1 foliation and stretching lineation. Furthermore, in the outcrop above Tällialp (Swiss coordinates 734750/152050) the F1 foliation and stretching linea-

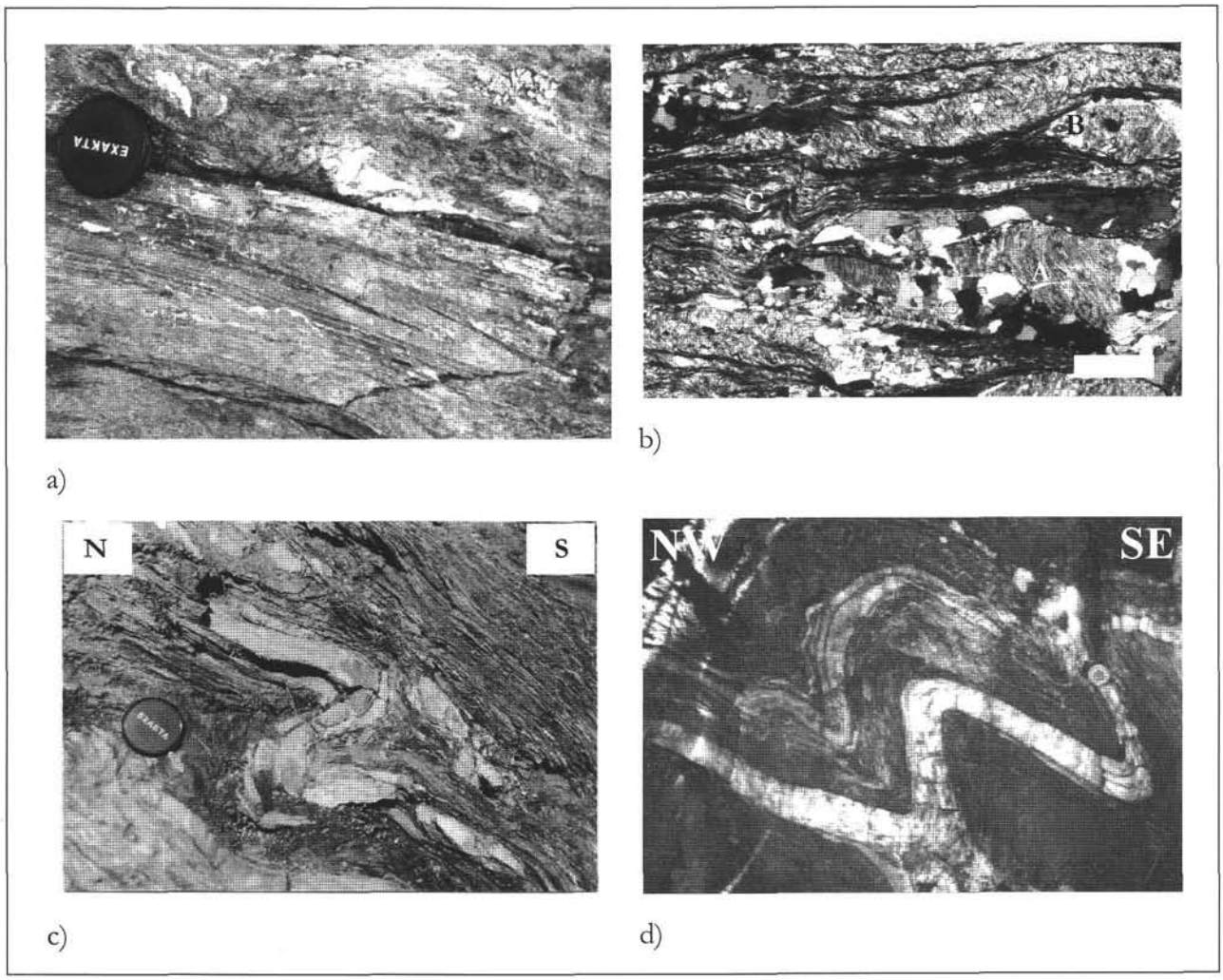

Fig 12
Deformation structures from the Misox zone and the Tambo nappe.
a) Isoclinal F1 (Ferrera phase) fold in Bündnerschiefer of the Misox zone (Upper Uccello zone). View towards SE. Fold axis is subparallel to the stretching lineation. Swiss coordinates 735 630/149 675.
b) F1 deformation: Thin section of Bündnerschiefer from the Misox zone (Upper Uccello zone) showing main F1 foliation (horizontal) and early F1 foliation (steep, folded). A: Folded internal foliation within and brittle fracture across albite grain; B: inclusion-free albite grown in strain shadow; C: Niemet-Beverin (F2) crenulation. Scale bar is 500 µm. Swiss coordinates 736 010/150 430.
c) F2 (Niemet-Beverin phase) fold in Bündnerschiefer of the Misox zone (Upper Uccello zone), folding the F1 foliation. Vergence towards south corresponds to the lower limb of the north-closing Niemet-Beverin megafold. Swiss coordinates 735 885/150 970.
d) North-vergent F3 (Domleschg phase) fold deforming mica schist of the Tambo nappe. Width of the picture is 60 cm. Swiss coordinates: 736 560/146 895.

tion can continuously be followed through the Pescion zone into the Adula nappe where these structures belong to the Zapport phase (D3).

F1 folds are always isoclinal and characterized by fold axial planes parallel to the F1 foliation (Fig. 12a). Within the study area, wavelengths and amplitudes do not exceed the order of a few dm and m, respectively. Fold axes trend either parallel or perpendicular to the F1 stretching lineation. Particularly in the latter case, the F1 mylonitic foliation is folded and a new axial planar foliation, being parallel to the former in the limbs, can be distinguished close to the fold hinges. On the other hand sporadically appearing intrafolial folds give examples of folds predating the shearing. Therefore, the Ferrera phase includes several episodes of repeated shearing and folding (see also MAYERAT DEMARNE 1994) which can readily be explained by its long duration (ca. 55-35 Ma; MARQUER et al. 1994).

Two F1 foliations also become visible in some thin-sections of samples from the Misox zone. The thin-section of a Bündnerschiefer from Val Vignun (Fig. 12b) may serve as an example. The main F1 foliation, made up by white mica and graphite, trends horizontally whereas an older foliation is outlined by white mica within the microlithons and by graphite and small inclusions in albite clasts. In this case the older foliation is probably connected with the occurrence of intrafolial folds in the outcrop where the sample was taken. Note the partly brittle deformation of albite (A) and that solution transfer processes contributed to the formation of the main foliation as can be seen from the dissolution of albite perpendicular to the main foliation and the growth of inclusion-free albite seams in strain shadows (B). The crenulation (C) of the main foliation is due to F2.

Although the F1 main foliation thus overprints earlier structures in some localities, we must forbear from defining subphases of F1 or even a new deformation phase since the above-mentioned multiform overprinting relations are local peculiarities that cannot be correlated among each other. Furthermore, all the described structures can be explained by ongoing north-vergent shearing. Note that the overprinting of early thrusts by Ferrera-phase folds has led to the definition of an Avers phase, predating the Ferrera phase, by MILNES and SCHMUTZ (1978). This phase, however, can only be clearly defined in the case of the detachment of the Avers Bündnerschiefer, east of our study area (SCHMID et al., 1997b).

4.3 F2/Niemet-Beverin phase

The main structure of the Niemet-Beverin phase is the Niemet-Beverin megafold by which the Schams nappes and part of the Bündnerschiefer are wrapped around the Briançonnais crystalline basement (MILNES and SCHMUTZ 1978, SCHMID et al. 1990, 1997b). The fold axial plane can be traced through the Suretta nappe where Ferrera phase isoclinal folds are refolded (SCHREURS 1995). Huge south vergent parasitic folds of the Niemet-Beverin fold in front of the Tambo nappe are spectacularly exposed in the western slope of the Guggernüll mountain (GANSSER 1937, MAYERAT DEMARNE 1994). The northern end of the eastern border of our study area corresponds roughly to the lower limb of the lowest of these folds whose axial plane strikes through the summit of Einshorn (Fig. 2) southward across Val Vignun.

Again parasitic folds of these occur within the parts of the Misox zone and the Tambo nappe that belong to the study area. They overprint F1 structures. While their wavelengths commonly lie within the order of a few dm, their amplitudes are quite variable. Tight to close folds (Fig. 12c) dominate within the Tambo nappe and upper parts of the Misox zone. In an overall view, F2 folds become more and more open and finally gentle towards the bottom of the Misox zone although their geometry also depends on the lithology. In some cases an F2 axial planar foliation cross-cutting the folded F1 foliation can be distinguished. Fold axes plunge to the east-northeast (maximum 72/27; Fig. 6h).

An F2 stretching lineation on the F1 foliation trends in the same direction as the fold axes (Fig. 6i). Parallelism between lineation and folds is directly observed where both occur. A south-vergent F2 crenulation of mica rich layers of Bündnerschiefer (Fig. 12b) runs parallel to the lineation and can in some occasions hardly be distinguished from it. The F2 stretching lineation is best developed in the Tambo nappe and the upper part of the Misox zone. C'-type shear bands indicate top-east-northeast movements. We interpret the reactivation of the F1 foliation as F2 shear plane to be caused by the rheologic anisotropy that resulted from F1 foliation. The generation of F2 folds may partly be due to the fact that the F2 deformation could not entirely be accommodated by shearing within the F1 foliation plane.

4.4 F3/Domleschg phase

F3 folds are common within the Tambo nappe and upper parts of the Misox zone but become scarce towards the lower Uccello zone. Their dimensions and geometries, including the orientation of fold axes (Fig. 6j), are comparable to those of close F2 folds from which the F3 folds (Fig. 12d) differ in being north-vergent. An F3 crenulation coaxial to F3 folds is developed within mica-rich layers of the Bündnerschiefer where it clearly overprints the S-vergent F2 crenulation. Apart from these folds, including here and there a fold axial planar foliation, no F3 related structures can be reported.

Folds similar to our F3 folds are widespread throughout the Suretta, Tambo and Schams nappes (MILNES and SCHMUTZ 1978, BAUDIN et al. 1993, MAYERAT DEMARNE 1994, SCHREURS 1995) and can be attributed to the Domleschg phase defined by PFIFFNER (1977) for the Bündnerschiefer of the Domleschg area.

4.5 F4

Within the Misox zone and the Tambo nappe flexures of the same kind and orientation as the D5 flexures of the Adula nappe affect mostly the competent rocks. They are best exposed east of the southern Piz Uccello summit where the surface is formed by the foliation of a thick layer of impure marble. In this outcrop the respective southern limbs are lowered by up to 2 m along the flexures. In other locations north-vergent flexures do also occur but less frequently. Overprinting relations of small-scale F4 flexures with preceding deformation phases can unambiguously be distinguished within incompetent layers of Bündnerschiefer where locally crenulations of F1, F2 and F3 coexist.

5. Tectonic evolution, time constraints, and metamorphism

The Early Eocene age (ZIEGLER 1956, EIERMANN 1988) of the latest sedimentation in the Valais ocean in eastern Switzerland signifies the beginning subduction of the Adula nappe whose position at that time was the distal European margin (SCHMID et al. 1990, 1997b). Due to the strong later overprint the prograde history of the Adula nappe remains rather obscure. According to LÖW (1987) the Sorreda phase imbrication and mylonitization took place under conditions of 6-8 kbar and 380-450° but it seems inevitable that similar deformations continued until the Trescolmen phase.

The high pressure metamorphism in the Adula nappe and the attached Cima Lunga unit has been dated by several authors: around 40 Ma (MURALT 1986), 48-39 Ma (SANTINI 1992), 40-35 Ma (BECKER 1993) and 35 Ma (GEBAUER 1996). Indeed, an age of about 40 Ma is likely since older ages would demand improbably high subduction rates and younger ages would not provide enough time for the exhumation of the Adula nappe below the Tambo nappe which must have ended earlier than 30 Ma (see below). HEINRICH (1986) recognized a strong pressure and a temperature gradient from north (ca. 13 kbar/500°) to south (ca. 30kbar/830°). Table 1 shows his results complemented by more recent data. However, one must not infer the dip angle of the subduction zone from the geobarometric data since the eclogitic boudins, from which the samples were taken, occupy different structural levels that were telescoped to a considerable amount by D3 imbricate stacking.

Contemporaneously with the Trescolmen phase in the mafic boudins, Zapport-phase overprint started in the surrounding rocks (e. g. LÖW 1987, MEYRE and PUSCHNIG 1993). Zapport-phase top-north shear movements led to an almost isothermal rapid decompression (PARTZSCH 1998, NAGEL 2000). At the end of the Zapport phase, a fair pressure gradient from north to south still existed. Minimal geothermobarometric data for the end of D3 yield 7 kbar/500° (LÖW 1987) for the north, 6.5-8.5 kbar/640-700° (PARTZSCH 1998) for the middle and 11-13 kbar/600-650° (NAGEL et al. 2002) for the south. By interpolation of the first two data sets the D3 conditions for the Adula nappe in the study area can be estimated at about 7kbar/550°. Our observations indicate a relatively low temperature at the end of the Zapport phase, because chlorite derived from garnet break-down occurs in some samples in strain shadows of garnet grains and along shear bands, indicating that at least a late stage of Zapport deformation proceeded when garnet was no longer stable. The results referred above are consistent with radiometric ages of non-eclogitic samples becoming progressively younger from north to south (see compilation and review in PARTZSCH 1998). Because the ages represent cooling ages (e. g. STECK and HUNZIKER 1994) they cannot directly be linked with D3. If temperatures slightly in excess of 500° are supposed for the study area, Rb-Sr white mica ages should, with respect to their closing temperature (500 ±50°; PURDY and JÄGER 1976), best approximate D3 ages; 43 ±9 Ma (JÄGER et al. 1967) and 36 ±4 Ma (MURALT 1986) have been obtained using this method on Adula rocks slightly north of the study area. The time span thus given can be reduced to 40-35 Ma if 40 Ma is assumed for the pressure peak and one takes into account that F2 must have ended earlier than 30 Ma (see below).

Our structural observations have shown that the F1 main foliation and stretching lineation of the Misox zone and Tambo nappe must definitely be correlated with the D3 foliation and stretching lineation. On the other hand, the structural ensemble of the Ferrera phase is much richer than that of the Zapport phase. No age data for the Misox zone are available. Age data of the Ferrera phase within the Suretta nappe, which underwent a similar history as the Tambo nappe (MARQUER et al. 1994), range from about 55 to 30 Ma: K-Ar amphibole ages of 55 ±1 Ma and 49 ±1 Ma on gneisses of the Suretta nappe are maximum F1 ages (HURFORD et al. 1989); K-Ar and Rb-Sr ages of white mica aligned in the F1 foliation plane range from 50 to 30 Ma (PURDY and JÄGER 1976, STEINITZ and JÄGER 1981, SCHREURS 1993, CHALLANDES 2000) and are interpreted as formation ages (HURFORD et al. 1989, SCHREURS 1993). Therefore, only late stages of the Ferrera phase can be correlated with the Zapport phase while earlier stages of the long-lasting heterogeneous Ferrera phase were coeval with the Sorreda and Trescolmen phases. Ages around 50 Ma suggest that the Briançonnais nappes entered the subduction zone earlier than the more external Adula nappe.

The F1 peak metamorphic conditions of the Tambo nappe have been determined based on the Si contents in phengite by BAUDIN and MARQUER (1993). Their results show increasing pressures and temperatures from 10 kbar/350° for the northern Tambo nappe to 13 kbar/550° for the south. Within the Misox zone TEUTSCH (1982) found for the Ferrera phase amphibolite facies conditions reaching from 6-8 kbar/600-660° in Val de la Forcola to 5-7 kbar/500-550° in the area around Mesocco

Table 1
Conditions of high-pressure metamorphism in the Adula nappe.

Northern Adula nappe	Vals	11-13 kbar / 450-550^0 (HEINRICH 1986) 12-15 kbar / 470-540^0 (LÖW 1987)	
Middle Adula nappe	Alp de Confin	12-22 kbar / 450-550^0 (HEINRICH 1986)	ca. 25 kbar / 600-650^0 (MEYRE et al. 1997)
	Alp de Trescolmen	and 15-22 kbar / 550-650^0 (HEINRICH 1986)	
Southern Adula nappe	Cima di Gagnone	15-25 kbar / 600-700^0 (HEINRICH 1986)	30 kbar / 740^0 (NIMIS & TROMMSDORFF 2001)
	Monte Duria	18-35 kbar / 750-900^0 (HEINRICH 1986)	30 kbar / 830^0 (NIMIS & TROMMSDORFF 2001)
	Alpe Arami		32 kbar / 840^0 (NIMIS & TROMMSDORFF 2001)

and greenschist facies conditions north of Mesocco. One glaucophane-bearing metabasalt in the Misox zone, 1 km north of our study area, yielded high-pressure conditions of >12 kbar and 460°-560° (RING 1992). With respect to the kinematic model developed below it is noteworthy that the peak pressures of the Adula nappe (ca. 25 kbar in our study area, MEYRE et al. 1997) by far exceed those of the higher units as well as those of the underlying Simano nappe (6-8 kbar; ENGI et al. 1995) and that the contact between the Adula nappe and Misox zone has not been significantly altered by post-Zapport deformations, at least in our study area.

In the Niemet-Beverin phase the north-directed shearing was replaced by west-east extension, occurring under 5-8 kbar/350-550° within the Tambo nappe (BAUDIN and MARQUER 1993). Vertical shortening of the units affected by F2 deformations led to the further exhumation of the nappe stack and the south-vergent folding at the base of the Tambo nappe and in the Misox zone (see also BAUDIN et al. 1993). The east directed shear movements affected all units between the Misox zone and the Turba mylonite zone at the bottom of the Platta unit. The Turba mylonite zone is truncated by the Bergell granodiorite (NIEVERGELT et al. 1996) whose emplacement is dated at 30 Ma (GULSON 1973, VON BLANCKENBURG 1992); hence a valuable time mark is given for the end of F2. Whereas macroscopic structures of the Niemet-Beverin phase die out towards the bottom of the Misox zone, the overprint of Zapport phase quartz textures by top-east rotation can, by comparison of strain orientations, only be ascribed to the Niemet-Beverin phase. This does not only put further emphasis on the statement that the Zapport phase predates the Niemet-Beverin phase (however, see e. g. PARTZSCH 1998 and SCHMID et al. 1996 for a differing view) but, moreover, provides a minimal time bracket for D3 (and F1) at about 35 Ma.

From structural observations in the study area no statement can be made on the age relation between the Leis phase and the Niemet-Beverin phase. Looking at results from the middle Adula nappe only, one might be tempted to regard the Leis phase as the weaker direct continuation of the Zapport phase under strongly heterogeneous, but still north-directed movements. However, NAGEL et al. (in press) point out that their D3, which they strongly assume to be identical with the Leis phase, affects the 30 Ma Bergell granodiorite whereas their D3 folds are truncated by the 24-25 Ma old Novate granite (LIATI et al. 2000). An age of about 30 to 25 Ma for the Leis phase has also been postulated by SCHMID et al. (1996) and PARTZSCH (1998) who correlate the Leis phase with the Domleschg phase of the higher units. This is confirmed by similar F3 ages reported by MARQUER et al. (1994) and the fact that our D4 and F3 exhibit reasonably similar structures.

Looking at geobarometric data, a severe change with respect to the preceding deformation phases can be stated in that the north-south pressure gradient in the Adula nappe no longer persists during the Leis phase: 7 kbar/500° for the north (LÖW 1987), 4.7-6.7 kbar/530-590° for the middle (PARTZSCH 1998) and 4-6 kbar/650-700° for the south of the nappe (NAGEL et al. 2002) on the contrary manifest an inversion of the pressure gradient. This differential uplift of the southern part of the nappe is acommodated by the D4 and F3 folds by which the respective northern parts are lowered.

The Carassino phase was accompanied by further exhumation leading to lower greenschist facies conditions (LÖW 1987, PARTZSCH 1998). It occurred at 25 to 20 Ma according to SCHMID et al. (1996). Contemporaneously or later (25-18 Ma; MEYRE et al. 1998) brittle-ductile deformation lowered the respective eastern sides along north-northwest-south-southeast striking normal faults, e. g. the Forcola fault. Within our study area late brittle deformation took place along north-northwest-south-southeast striking quartz veins at which the respective western sides were lowered by obviously only small amounts in the sense of normal faulting. These minor faults are probably related to the Forcola normal fault which, however, does not continue as a major fault into our study area.

6. A kinematic scenario for eclogite exhumation in the Adula nappe

The eclogite-bearing Adula nappe is overlain and underlain by the Tambo nappe and the Simano nappe, respectively, in both of which no eclogites have been found so far. It appears that the Misox zone is free of eclogite as well; at least in the study area, we did not find any eclogite or retrograded eclogite in the Misox zone. A glaucophane-bearing metabasite is reported from a locality in the Misox zone 1 km north of our study area (GANSSER 1937). Within the Adula nappe, the eclogites appear to be restricted to the upper part of the nappe (PARTZSCH 1998). Hence, the eclogites (and, in the southern part of the nappe, garnet peridotites) are found in a sheet only a few km thick but 50 km long in north-south-direction. This eclogite-bearing sheet is composed of a multitude of gneiss lenses imbricated in the way of a forward-dipping duplex (Fig. 4; JENNY et al. 1923). Petrological work (MEYRE et al. 1999a, NAGEL 2000) has shown that the gneissic country rocks of the eclogite boudins suffered comparable pressures as the eclogites. Current models for eclogite exhumation (e. g., CHEMENDA 1995, ERNST 1999) assume that such sheets of high-pressure rocks are emplaced between lower-pressure rocks by the contemporaneous action of normal-sense shear zones at the top and reverse-sense shear zones at the base of the sheet. For the Adula nappe, which had been subducted towards south as indicated by the southward increase of peak pressures, such models would predict a top-south normal shear zone in the roof of the nappe. This is clearly not the case here, since all the shear-sense criteria related to the main deformation phase (Zapport phase) in the study area indicate top-north transport of the Misox zone and the Tambo nappe over the Adula nappe. With respect to the south-dipping subduction zone, this shear zone has a thrust orientation. Nevertheless, shearing during the Zapport phase accommodated the main part of the exhumation of the Adula rocks.

This paradoxical situation may be explained if we assume that the eclogite-bearing sheet was exhumed from below into a top-north shear zone, as shown in Fig. 13. In this figure, a speculative scenario is developed which, at the present state of knowledge, appears to be the most suitable to explain the structural and tectonometamorphic evolution. It is based on the reconstruction of SCHMID et al. (1996), but with one important modification: We assume that for some

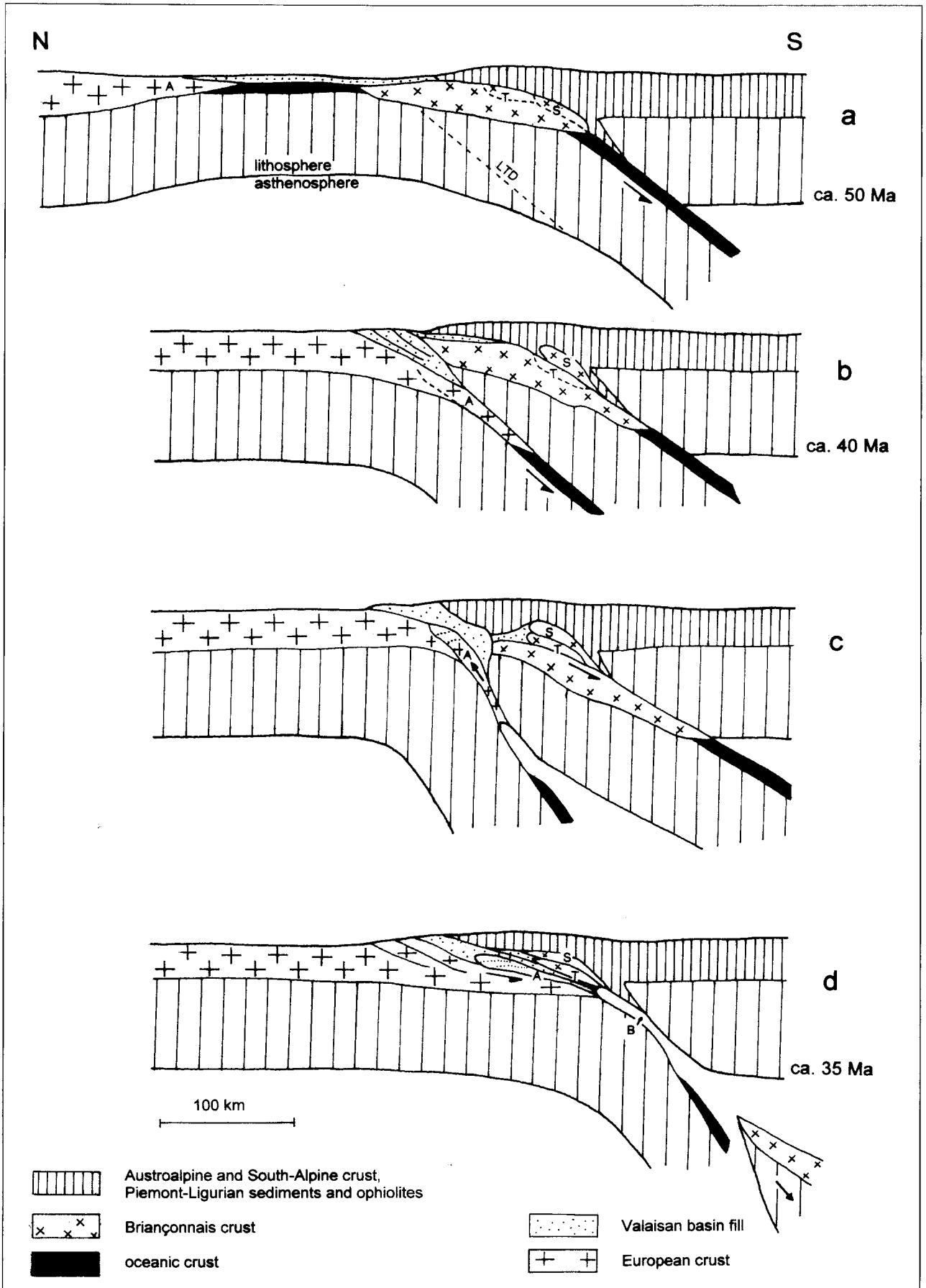
N
S
a
lithosphere
asthenosphere
LTD
ca. 50 Ma
b
ca. 40 Ma
c
d
ca. 35 Ma
100 km
Austroalpine and South-Alpine crust,
Piemont-Ligurian sediments and ophiolites
Briançonnais crust
oceanic crust
Valaisan basin fill
European crust

time between 50 and 35 Ma, the Valais ocean formed an independent downgoing slab, in addition to the Piemont-Ligurian slab further south (see also PFIFFNER et al., 2000, Fig. 13). At ca. 50 Ma, the Piemont-Ligurian oceanic lithosphere had been subducted southward under the Adriatic continental margin so that the Briançonnais microcontinent collided with that margin (Fig. 13a). As a result of this collision, the Piemont-Ligurian subduction zone became (temporarily) locked and subduction of the Valaisan oceanic lithosphere started further north. The location where the lithosphere broke and the new subduction zone was installed may have been predetermined by a rifting-related, Jurassic-age detachment fault dipping southeast under the Briançonnais continent. Such a detachment fault is preserved farther east, in the Engadine window (Lower Tasna detachment of FROITZHEIM and RUBATTO 1998; LTD in Fig. 13a). When the Valaisan lithosphere had been consumed, the thinned European continental margin (Adula nappe) descended in the subduction zone, forming a duplex of basement and cover rocks (Sorreda phase). Subduction led to peak pressure in the Adula rocks around 40 Ma (Fig. 13b). When, after the thinned European margin, the normal-thickness European continental crust entered the subduction zone, this northern subduction became locked. Further convergence was accommodated by a reactivation of the southern subduction zone, possibly because now less work had to be done to subduct the thinned crust of the Briançonnais than would have been necessary for subducting the normal crust of the European margin. This time, however, the main subduction thrust did not follow the top of the Briançonnais basement but made a short-cut through that basement, below the Tambo and Suretta nappes which were thus accreted to the hanging wall (Fig. 13c; see also Fig. 12 in PFIFFNER et al., 2000). At that stage, the Adula nappe and the Suretta and Tambo nappes were separated by a wedge of Briançonnais lower crust and mantle. The presence of this wedge, which was later removed, explains the southward-increasing pressure gap between the Adula nappe and the Tambo nape: In the north, the wedge was only narrow and the pressure gap small, whereas towards south its thickness increased, and so does the pressure gap. In the south, the peak pressures are 30 kbar for Monte Duria in the Adula nappe (NIMIS and TROMMSDORFF 2001) and 13 kbar for the southern Tambo nappe (BAUDIN and MARQUER 1993) corresponding to a pressure difference of 17 kbar, or a depth difference of 50 km.

From now on, the deeper Briançonnais basement, the European margin and the Adula rocks were underthrust together towards south under the orogenic wedge. At first, this may have led to further burial and pressure increase of the Adula rocks. We speculate that at some point the Briançonnais lower crust and mantle, with the dense Piemont-Ligurian slab still attached to it, accelerated its descent and began to sink off into the deeper mantle. By this process, the old Valaisan subduction channel enclosing the Adula duplex became extended and the Adula nappe was released to begin its ascent, possibly partly driven by buoyancy of the crustal gneisses relative to the bordering mantle rocks (Fig. 13c). In this stage, a top-south shear zone must have existed in the roof of the Adula nappe, but ist structures have been completely erased during subsequent, D3, top-north shearing. The highly ductile Adula material was exhumed into the top-north shear zone along which the European margin was thrust under the Tambo and Suretta nappe. This caused the pervasive Zapport-phase deformation of the Adula gneisses together with the overlying Misox and Tambo rocks (Fig. 13d). When the Adula rocks entered the top-north shear zone, they were continuously accreted to the hanging wall, so that further top-north thrusting did not result in their renewed burial and pressure increase. We assume that the peridotite bodies in the Adula nappe, like Alpe Arami, Cima di Gagnone, Monte Duria and, in our study area, Sass de la Golp represent traces of the now disappeared Briançonnais mantle. The fact that the Sass de la Golp peridotite contains olivine (HUNDENBORN 2001) suggests its origin from mantle and not from oceanic crust, because in the case of oceanic crust the olivine would probably have been replaced by serpentine.

This three-plate scenario (Adria, Briançonnais, Europe) allows unroofing the Adula nappe during ongoing overall convergence between Europe and Adria, as required by plate tectonic reconstructions (see SCHMID et al. 1996). Still, there is some component of extension involved in the scenario, but this extension occurs in the subsurface between slowly-descending Europe and more rapidly-descending Briançonnais.

In the Niemet-Beverin phase, postdating the Zapport phase, the study area was affected by a certain amount of east-west extension. This deformation occurred when the Adula eclogites had already been substantially exhumed and emplaced below the Tambo nappe. Top-north shearing during the Zapport phase already accommodated exhumation of the Adula nappe to greenschist-facies conditions, as is demonstrated by chlorite growth along shear bands and in garnet tails during the Zapport phase (see above). Additional exhumation of the Adula nappe together with the Tambo and Suretta nappes was indeed accommodated by the Niemet-Beverin phase. The major top-east to top-southeast shear zone which formed during the Niemet-Beverin phase (see SCHMID et al. 1990, 1997b, NIEVERGELT et al. 1996, NAGEL 2000) passes over the study aera in a higher structural level. This leads to an upward increase in the intensity of Niemet-Beverin deformation in the study area. Whereas in the Adula nappe this deformation is only very weak, it becomes pronounced in the Areua and Schams slices at the front of the Tambo nappe where a clear Niemet-Beverin stretching lineation can be found. Only in the southern part of the Adula nappe, near the Insubric line, did the shear zone strongly affect and refold this nappe (NAGEL 2000).

← Fig. 13
Sequence of hypothetical cross-sections showing the burial and exhumation of the Adula eclogites in the framework of the Tertiary Alpine continent collision. A: Adula; B: ascending Bergell melt; LTD: approximate location of Jurassic-age, rifting-related detachment fault corresponding to the Lower Tasna Detachment (FROITZHEIM & RUBATTO 1998); S: Suretta nappe; T: Tambo nappe. No vertical exaggeration.

7. Acknowledgments

We thank Thorsten NAGEL, Stefan SCHMID, and Dieter GEBAUER for discussions and suggestions, and Adrian PFIFFNER and Guido SCHREURS for careful and constructive reviews. The work of Walter KURZ was supported by an Erwin SCHRÖDINGER research fellowship (J1986-GEO, J2155-GEO) of the Austrian Science Fund (FWF).

References

BABINKA, S., 2001: Geologische und strukturelle Kartierung des Gebietes südlich von San Bernardino. – Unpubl. diploma mapping report, Bonn University.

BAUDIN, T., MARQUER, D. & PERSOZ, F., 1991: New lithological and structural results in the Tambo nappe, Central Alps, Switzerland. – Terra Abstr. **3** (1), 222.

BAUDIN, Th. & MARQUER, D., 1993: Métamorphisme haute pression dans la nappe de Tambo (Alpes centrales Suisses): utilisation du geobaromètre phengitique. – Schweiz. mineral. petrogr. Mitt. **73,** 285-300.

BAUDIN, T., MARQUER, D. & PERSOZ, F., 1993: Basement-cover relationships in the Tambo nappe (Central Alps, Switzerland): geometry, structures and kinematics. – J. Struct. Geol. **15** (3/5), 543-553.

BAUMGARTNER, L. B. & LÖW, S., 1983: Deformation und Metamorphose der Adula-Decke südwestlich San Bernardino. – Schweiz. mineral. petrol. Mitt. **63,** 215-232.

BECKER, H., 1993: Garnet peridotite and eclogite Sm-Nd mineral ages from the Lepontine dome (Swiss Alps): New evidence for an Eocene high-pressure metamorphism in the Central Alps. – Geology **21,** 599-602.

BOYER, S. E. & ELLIOTT, D., 1982: Thrust systems. – AAPG Bull. **66,** 1196-1230.

CHALLANDES, N., 2000: Comportement des systèmes isotopiques 39Ar-40Ar et Rb-Sr dans les zones de cisaillement: Exemples du massif de l'Aar (Massifs cristallins externes) et de la nappe de Suretta (Alpes centrales suisses). – Unpubl. Ph.D. thesis, University Neuchâtel.

CHEMENDA, A. I., MATTAUER, M., MALAVIEILLE, J. & BOKUN, A. N., 1995: A mechanism for syn-collisional rock exhumation and associated normal faulting: Results from physical modelling. – Earth Planet. Sci. Lett. **132,** 225-232.

EGLI, W., 1966: Geologisch-petrographische Untersuchungen in der NW-Aduladecke und in der Sojaschuppe (Bleniotal, Kanton Tessin). – Mitt. geol. Inst. ETH u. Univ. Zürich [Neue Folge] 47.

EIERMANN, D. R., 1988: Zur Stellung des Martegnas-Zuges. – Eclogae geol. Helv. **81,** 259-272.

ENGI, M., TODD, C. S. & SCHMATZ, D. R., 1995: Tertiary metamorphic conditions in the eastern Lepontine Alps. – Schweiz. mineral. petrogr. Mitt. **75,** 347-369.

ERNST, W. G., 1999: Metamorphism, partial preservation, and exhumation of ultrahigh-pressure belts. – The Island Arc **8,** 125-153.

FLORINETH, D. & FROITZHEIM, N., 1994: Transition from continental to oceanic basement in the Tasna nappe (Engadine window, Graubünden, Switzerland): Evidence for Early Cretaceous opening of the Valais ocean. – Schweiz. mineral. petrogr. Mitt. **74,** 437-448.

FROITZHEIM, N., SCHMID, S. M. & FREY, M., 1996: Mesozoic paleogeography and the timing of eclogite-facies metamorphism in the Alps: a working hypothesis. – Eclogae geol. Helv. **89,** 81-110.

FROITZHEIM, N. & RUBATTO, D., 1998: Continental breakup by detachment faulting: field evidence and geochronological constraints (Tasna nappe, Switzerland). – Terra Nova **10,** 171-176.

GANSSER, A., 1937: Der Nordrand der Tambodecke. – Schweiz. mineral. petrogr. Mitt. **17,** 291-522.

GEBAUER, D., 1996: A P-T-t path for (ultra?-) high-pressure ultramafic/mafic rock-association and their felsic country-rocks based on SHRIMP-dating of magmatic and metamorphic zircon domains. Example: Alpe Arami (Central Swiss Alps). – In: BASU, A. & HART, S. R. (eds): Earth Processes: Reading the Isotopic Code. – Geophys. Monogr. Ser. 95.

GODARD, G. & VAN ROERMUND, H. L. M., 1995: Deformation-induced clinopyroxene fabrics from eclogites. – J. Struct. Geol. **17,** 1425-1443.

GULSON, B. L., 1973: Age relations in the Bergell region of the southeast Swiss Alps: with some geochemical comparisons. – Eclogae geol. Helv. **66/2,** 293-313.

HÄNNY, R., GRAUERT, B. & SOPTRAJANOVA, G., 1975: Paleozoic migmatites affected by high-grade Tertiary metamorphism in the Central Alps (Valle Bodengo, Italy). A geochronological study. – Contr. Mineral. Petrol. **51,** 173-196.

HANSON, G., GRÜNENFELD, M. & SOPTRAYANOVA, G., 1969: The geochronology of a recrystallized tectonite in Switzerland – the Rofna gneiss. – Earth and planet. Sci. Lett. **5/6,** 413-422.

HEINRICH, C. A., 1986: Eclogite facies regional metamorphism of hydrous mafic rocks in the Central Alpine Adula nappe. – J. Petrol. **27,** 123-154.

HELMSTAEDT, H., ANDERSON, O. L. & GAVASCI, A. T., 1972: Petrofabric studies of eclogite, spinel-websterite and spinel-lherzolith xenoliths from kimberlite-bearing breccia pipes in southeastern Utah and north-eastern Arizona. – J. geophys. Res. **77,** 4350-4365.

HUNDENBORN, R., 2001: Entstehung, Metamorphose und Deformation der basischen und ultrabasischen Gesteine in der Adula-Decke und der Misoxer Zone, unter besonderer Berücksichtigung der Adula-Eklogite. – Unpubl. diploma thesis, Bonn University.

HUNZIKER, J. C., DESMONS, J. & HURFORD, A. J., 1992: Thirty-two years of geochronological work in the Central and Western Alps: a review on seven maps. – Mém. Géol. Lausanne 13.

HURFORD, A. J., FLYSCH, M. & JÄGER, E., 1989: Unravelling the thermo-tectonic evolution of the Alps: A contribution from fission track analysis and mica dating. – In: COWARD, M., DIETRICH, D. & PARK, R. G. (eds.): Alpine Tectonics. – Spec. Publ. Geol. Soc. London **45,** 369-398.

JÄGER, E., NIGGLI, E. & WENK, E., 1967: Altersbestimmungen an Glimmer der Zentralalpen. – Beitr. geol. Karte Schweiz [Neue Folge] 134.

JANSEN, E., SCHÄFER, W. & KIRFEL, A., 2000: The Jülich neutron diffractometer and data processing in rock texture investigations. – J. Struct. Geol. **22,** 1559-1564.

JENNY, H., FRISCHKNECHT, G. & KOPP, J., 1923: Geologie der Adula. – Beitr. geol. Karte Schweiz [Neue Folge] 51.

KREMER, K., 2001: Geologische und strukturelle Kartierung des Gebietes um San Bernardino (Graubünden/Schweiz). – Unpubl. diploma mapping report, Bonn University.

KÜNDIG, E., 1926: Beiträge zur Geologie und Petrographie der Gebirgskette zwischen Val Calanca und Misox. – Schweiz. mineral. petrogr. Mitt. **4,** 1-99.

LIATI, A., GEBAUER, D. & FANNING, M., 2000: U-Pb SHRIMP dating of zircon from the Novate granite (Bergell, Central Alps): evidence for Oligocene-Miocene magmatism, Jurassic/Cretaceous continental rifting and opening of the Valais trough. – Schweiz. mineral. petrogr. Mitt. **80,** 305-316.

LINIGER, M., 1992: Der ostalpin-penninische Grenzbereich im Gebiet der Nördlichen Adula-Decke Margna-Decke (Graubünden, Schweiz). – Unpubl. Ph.D. thesis, ETH Zürich.

LÖW, S., 1987: Die tektono-metamorphe Entwicklung der nördlichen Adula-Decke. – Beitr. geol. Karte Schweiz [Neue Folge] 161.

MARQUER, D., 1991: Structures et cinématique des déformations dans le granite de Truzzo (Nappe de Tambo, Alpes centrales suisses). – Eclogae geol. Helv. **84/1,** 107-123.

MARQUER, D., BAUDIN, T., PEUCAT, J.-J. & PERSOZ, F., 1994: Rb-Sr mica ages in the alpine shear zones of the Truzzo granite: Timing of the Tertiary alpine P-T-deformations in the Tambo nappe (Central Alps, Switzerland). – Eclogae geol. Helv. **87/1,** 225-239.

MAYERAT DEMARNE, A.-M., 1994: Analyse structurale de la zone frontale de la nappe du Tambo (Pennique, Grisons, Suisse). – Matér. Carte géol. Suisse [nouvelle série] 165.

MEYRE, C., DE CAPITANI, C., ZACK, T. & FREY, M., 1999a: Petrology of high-pressure metapelites from the Adula nappe (Central Alps, Switzerland). – Journal of Petrology **40,** 199-213.

MEYRE, C., DE CAPITANI, C. & PARTZSCH, J. H., 1997: A ternary solid solution model for omphacite and its application to geothermobarometry of eclogites from the Middle Adula nappe (Central Alps, Switzerland). – J. metamorphic Geol. **15,** 687-700.

MEYRE, C., MARQUER, D., SCHMID, S. M. & CIANCALEONI, L., 1999b: Syn-orogenic extension along the Forcola fault. – Eclogae geol. Helv. **91,** 409-420.

MEYRE, C. & PUSCHNIG, A. R., 1993: High-pressure metamorphism and deformation at Trescolmen, Adula nappe, Central Alps. – Schweiz. mineral. petrogr. Mitt. **73,** 277-283.

MEZGER, K., HANSON, G. N. & BOHLEN, S. R., 1989: High-precision U-Pb ages of metamorphic rutile: application to the cooling history of high-grade terranes. – Earth and planet. Sci. Lett. **96,** 106-118.

MILNES, A. G. & SCHMUTZ, H. U., 1978: Structure and history of the Suretta nappe (Pennine Zone, Central Alps) – a field study. – Eclogae geol. Helv. **71/1,** 19-23.

MURALT, R., 1986: Mineralogisch-geologische Untersuchungen in der Adula-Decke am Nordhang des San Bernardino-Passes (Graubünden, Schweiz). – Unpubl. diploma thesis, University Bern.

NABHOLZ, W., 1945: Geologie der Bündnerschiefergebirge zwischen Rheinwald, Valser- und Safiental. – Eclogae geol. Helv. **38/1,** 1-120.

NAGEL, T., 2000: Metamorphic and structural history of the southern Adula nappe (Graubünden, Switzerland). – Unpubl. Ph.D. thesis, Basel University.

NAGEL, T., DE CAPITANI, C., & FREY, M., 2002: Isograds and P-T evolution in the eastern Lepontine Alps (Graubünden, Switzerland). – J. Metamorph. Geol. **20,** 309-324.

NAGEL, T., DE CAPITANI, C., FREY, M., STÜNITZ, H., SCHMID, S. M. & FROITZHEIM, N., (in press) : Structural and metamorphic evolution during rapid exhumation of the southern Simano and Adula nappes (Central Alps, Switzerland). – Eclogae geol. Helv.

NEUMANN, B., 2000: Texture development of recrystallised quartz polycrystals unravelled by orientation and misorientation characteristics. – J. Struct. Geol. **22,** 1695-1711.

NIEVERGELT, P., LINIGER, M., FROITZHEIM, N. & FERREIRO MÄHLMANN, R., 1996: Early to mid Tertiary crustal extension in the Central Alps: The Turba Mylonite Zone (Eastern Switzerland). – Tectonics **15,** 329-340.

NIMIS, P. & TROMMSDORFF, V., 2001: Revised thermobarometry of Alpe Arami and other garnet peridotites from the Central Alps. – Journal of Petrology **42,** 103-115.

PANOZZO, R., 1983: Two-dimensional analysis of shape-fabric using projections of digitized lines in a plane. – Tectonophysics **95:** 279-294

PANOZZO, R., 1984: Two-dimensional strain from the orientation of lines in a plane. – J. Struct. Geol. **6,** 215-221

PARTZSCH, J. H., 1998; The tectono-metamorphic evolution of the middle Adula nappe, Central Alps, Switzerland. – Unpubl. Ph.D. thesis, University Basel.

PFIFFNER, O. A., 1977: Tektonische Untersuchungen im Infrahelvetikum der Ostschweiz. – Mitt. geol. Inst. ETH u. Univ. Zürich [N. F.] 217.

PFIFFNER, O. A., ELLIS, S. & BEAUMONT, C., 2000: Collision tectonics in the Swiss Alps: Insight from geodynamic modeling. – Tectonics **19,** 1065-1094.

PLEUGER, J., 2001: Strukturgeologische Untersuchungen in der Aduladecke, Misoxer Zone und Tambodecke am Passo del San Bernardino. – Unpubl. diploma thesis, Bonn University.

PLEUGER, J., JANSEN, E., SCHÄFER, W., OESTERLING, N. & FROITZHEIM, N., 2002: Neutron texture study of a natural gneiss mylonite affected by two phases of deformation. – Applied Physics A, **74** [Suppl.], 1058-1060.

PURDY, J. W. & JÄGER, E., 1976: K-Ar ages on rock-forming minerals from the Central Alps. Mem. Ist. – Geol. Mineral. Univ. Padova 30.

RING, U., 1992: The Alpine geodynamic evolution of Penninic nappes in the eastern Central Alps: geothermobarometric and kinematic data. – J. metamorph. Geol. **10,** 33-53.

RÜCK, P., 1995: Stratigraphisch-sedimentologische Untersuchung der Schamser Decken. In: Die Schamser Decken, part 1. – Beitr. geol. Karte Schweiz [Neue Folge] 167.

SANTINI, L., 1992: Geochemistry and geochronology of the basic rocks of the Penninic Nappes of East-Central Alps (Switzerland). – Unpubl. Ph.D. thesis, University Lausanne.

SCHMID, S. M., PFIFFNER, O. A., FROITZHEIM, N., SCHÖNBORN, G. & KISSLING, E., 1996: Geophysical-geological transect and tectonic evolution of the Swiss-Italian Alps. – Tectonics **15,** 1036-1064.

SCHMID, S. M., PFIFFNER, O. A., SCHÖNBORN, G., FROITZHEIM, N., & KISSLING, E., 1997a: Integrated cross section and tectonic evolution of the Alps along the Eastern Traverse. – In: PFIFFNER, O. A., LEHNER, P., HEITZMANN, P., MUELLER, S. & STECK, A. (eds.): Deep structure of the Swiss Alps. Birkhäuser, Basel, 289-304.

SCHMID, S. M., PFIFFNER, O. A. & SCHREURS, G., 1997b: Rifting and collision in the Penninic zone of eastern Switzerland. – In: PFIFFNER, O. A., LEHNER, P., HEITZMANN, P., MUELLER, S. & STECK, A. (eds.): Deep structure of the Swiss Alps. Birkhäuser, Basel, 160-185.

SCHMID, S. M., RÜCK, P. & SCHREURS, G., 1990: The significance of the Schams nappes for the reconstruction of the paleotectonic and orogenic evolution of the Penninic zone along the NFP-20 East traverse (Grisons, eastern Switzerland). – Mém. Soc. géol. France **156,** 263-287.

SCHREURS, G., 1993: Structural analysis of the Schams nappes and adjacent tectonic units. Implications for the orogenic evolution of the Penninic zone in Eastern Switzerland. – Bull. Soc. géol. Fr. **164 (3),** 425-435.

SCHREURS, G., 1995: Geometry and kinematics of the Schams nappes and adjacent tectonic units in the Penninic zone. In: Die Schamser Decken, part 2. – Beitr. geol. Karte Schweiz [Neue Folge] 167.

SPICHER, A., 1980: Tektonische Karte der Schweiz (1:500000). – Schweiz. Geol. Komm.

STAMPFLI, G., 1993: Le Briançonnais, terrain exotique dans les Alpes?. – Eclogae geol. Helv. **86,** 1-45.

STAMPFLI, G., MOSAR, J., MARQUER, D., MARCHANT, R., BAUDIN, T. & BOREL, G., 1998: Subduction and obduction processes in the Swiss Alps. – Tectonophysics **296,** 159-204.

STECK, A. & HUNZIKER, J., 1994: The Tertiary structural and thermal evolution of the Central Alps. Compressional and extensional structures in an orogenic belt. – Tectonophysics **238,** 229-254.

STEINITZ, G. & JÄGER, E., 1981: Rb-Sr and K-Ar studies on rocks from the Suretta Nappe; Eastern Switzerland. – Schweiz. mineral. petrogr. Mitt. **61,** 121-131.

STEINMANN, M., 1994: Ein Beckenmodell für das Nordpenninikum der Ostschweiz. – Jahrb. Geol. Bundesanst. Wien **137,** 675-721.

STROHBACH, H., 1965: Der mittlere Abschnitt der Tambodecke samt seiner mesozoischen Unterlage und Bedeckung. – Mitt. geol. Inst. ETH u. Univ. Zürich [Neue Folge] 38.

TEUTSCH, R., 1982: Alpine Metamorphose der Misoxer Zone (Bündnerschiefer, Metabasite, granitische Gneise). – Unpubl. Ph.D. thesis, University Bern.

VAN DER PLAS, L., 1959: Petrology of the northern Adula region, Switzerland (with particular reference to the glaucophane-bearing rocks). – Leidse geol. Meded. **24/2,** 413-603.

VON BLANCKENBURG, F., 1992: Combined high-precision chronometry and geochemical tracing using accessory minerals: Applied to the Central-Alpine Bergell intrusion (central Europe). – Chem. Geol. **100,** 19-40.

WENK, H.-R., MATTHIES, S., DONOVAN, J. & CHATEIGNER, D., 1998: BEARTEX, a Windows-based program system for quantitative texture analysis. – J. Appl. Cryst. **31,** 262-269.

ZIEGLER, W., 1956: Geologische Studien in den Flyschgebieten des Oberhalbsteins (Graubünden). – Eclogae geol. Helv. **49/1,** 1-78.

Manuscript received: 27. 03. 2002
Revised version received: 20. 12. 2002
Manuscript accepted: 03. 01. 2003